LIFE NIEBLAS Final Report

Work carried out by the ICIA personnel involved

Action C.1: Innovation on fog collectors. Monitoring and evaluation protocol

Compiled by Life-Nieblas team: Instituto Canario de Investigaciones Agrarias (ICIA)

Due Date: 14/10/2024

Delivery Date: 03/2025

Content

1. Brief

Life Nieblas is a Life Programme financed project provided by the European Commission that support projects involved in climate action, natural habitat restoration and sustainable development. In addition to the European financing, Life Nieblas counts with the financial support from Cabildo de Gran Canaria as the public administration where this project has being developed.

Life Nieblas is a pioneer case study on the use of fog water collection as main source of water supply for the irrigation and maintenance of reforested areas. Reforestation methods will take shape of different technologies that have been observed to be beneficial or that have the potential to be further developed including: Individual Fog Water Collectors, Cocoons (developed in another Life project 'The Green Link'), AFDS (Autonomous Fluid Discharge System) and finally traditional reforestation as control group.

Furthermore, Life Nieblas looks into the transferability and replication potential of the technology tested. Not only will the project focus on the reforestation aspect but also on Fog Water Collectors (FWC) technology as the main (and only) source of water. In this case, technology has been tested in labs to improve FWC design and efficiency, they will not only become easier to install and transport but also will collect more water by surface exposed.

The final objective of this project will be to adapt technology to be exported to different European regions (and out of the EU) where fog conditions have the potential to improve water availability and assist in natural habitat recovery. Eventually, finding transferability into the agriculture sector where farmers can take advantage from collecting their own water. Henceforth, Life Nieblas will contribute in climate change mitigation action (by reduction of emissions), carbon capture (by natural habitat recovered) and with the development of sustainable technology.

2. Summary

Water scarcity in dry regions affected by low clouds has motivated exploring strategies for obtaining fresh water from humid air. However, water harvesting with conventional fog water collectors (FWC) is subjected to many limitations. Traditional devices are inefficient and structurally unstable under strong winds. Also, deployment in the field is difficult. This has limited their wider spread use and it is one of the main reasons for the long-term failure of fog water harvesting projects. Within the framework of LifeNieblas, under Action C1, we have designed an innovative fog water collector (i-FWC) that aims resolving many of these limitations using 3D printing techniques. It is shown that collected fog water droplets are quickly evacuated and do not clog the devised screen, maximising fog water yields. Also, due to its 3D geometry, the new design is less affected by changes in wind direction and gusts, whereas its field display is facilitated. This i-FWC will be associated to individual plantlets in the reforestation area in order to improve their survival rate.

This document describes the methods and instrumentation used to design, fabricate and test the different prototypes devised. Both lab and field experimental results aimed to maximising their fog water collection yield are shown. The main results and goals achieved are summarised in the following sections. Further information is included in Appendix I-IV. Additional audiovisual material may be accessed at:
https://drive.google.com/drive/folders/1gF5OS_m4XYs7CV4SkD7zJOZ3yB0DrgAN

3. Motivation and state of the art

Traditional methods to collect fog water basically consist of a screen facing the prevailing wind direction. Fog water droplets (of the order of 1-50 µm) blown by the air are thus intercepted by the mesh due to their inertia; further droplets impinge and join those already adhered to the screen to form larger drops; and these slide along the mesh elements, falling under the influence of gravity into a trough or gutter, and are conveyed to a storage tank. Consequently, collection efficiency depends greatly on the speed and size of the water droplets (more specifically on the Stokes and Reynolds numbers), as well as the geometry and wettability of the obstacle, and therefore the characteristics of the impacting surface. More importantly, aerodynamic effects play a significant role, as moist air has to cross a screen that interrupts its free-flowing path. Both impaction and aerodynamic characteristics must therefore be fine-tuned in order to maximize the collection efficiency. A very sealed knitted structure would improve impaction but in detriment of the poor aerodynamics of a blunt obstacle. In other words, a fog collector works basically as a filter: a thick filter would retain most of the particles in the stream but does not permit free flow, while a loose open filter would allow rapid cross-flow but with low retention capacity. An additional complication of fog “filtering” is that, captured fog water drops may be lost by re-entrainment back into the wind stream under strong gusts.

Thus, many parameters affect the collection of fog water. On the fog water collector’s side, the diameter, geometry and orientation of the impacting mesh filaments, the mesh shading (i.e., percentage of area covered by the solid screen) and number of collecting layers are the main aspects to be considered. Also, the material of the screen and its surface characteristics (wettability, adhesion) are relevant. From the point of view of the fog stream, the liquid water content, size of fog water droplets and wind velocity are relevant issues to take into account. Fog liquid water content represents only an amount of the order of 0.1–1.25 grams of water per cubic meter of air, and it is determined by the density and size distribution of the fog droplets. Liquid water content thus limits the potential (maximum) volume of water that can be obtained from the fog.

Given these requirements, i.e., sufficient wind speed, high liquid water content, appropriate size of the impaction elements and fog droplets, different collectors can be devised for capturing fog water artificially. In this respect, fog water gauges are usually either three-dimensional (thus fairly independent of wind direction) or flat structures provided with some kind of mesh or vertical filament array. Artificial fog water collectors have typical capturing surfaces of the order of a few square meters (0.5–10 m^2). Given the rather low water yields usually obtained by artificial means, low-tech designs, such as framed mesh screens held by two poles, have prevailed over more sophisticated collectors in practical applications. Accordingly, their maintenance is minimal, however the mesh and foundations may be damaged because of wind forces. An alternative to resolve these issues has been the use of parallelepiped and more complex 3D shapes at the expense of an increase in costs and difficulty of field deployment, and consequently their less frequent presence in previous projects. Other disadvantages of FWC include their dependence on the meteorological conditions and the topography of the area, and thus their reduced reliability when a constant fog water supply is desired.

Several studies around the World have reported daily fog water collection yields ranging from 0.2 to 4 $L \cdot m^{-2} \cdot d^{-1}$. As mentioned above, the collection capacity of a particular mesh structure depends on its design, but it is also strongly influenced by the speed of winds blowing normal to the collection surface, thus the comparison or extrapolation of these values to other scenarios may be challenging, because different fog conditions, collection periods, and mesh designs have been used in these studies. Another issue that is usually obviated in many fog harvesting projects is the total cost of the installation and, therefore, comparisons among these are not straightforward. In this regard, storage, pumping and distribution of the collected water is generally not specified, despite it represents the most expensive and troublesome part of the installation.

4. Objectives

The objective of the current project action is to develop a fog water collector *ad hoc* for providing water to plantlets of reforested *laurisilva* trees in Valleseco, El Andén (Gran Canaria) in order to improve their survival rate. The design will be based on first principles of fog droplets impaction and aerodynamics of permeable screens, in order to maximise water yields. Modular scalability, self-ground-sustenance, self-mounting, lightness and portability will be criteria taken into account to overcome some of the disadvantages of current FWC. Experiments were carried out in a wind tunnel where artificial fog was generated in order to fine-tune the characteristics of the screen. Also, some computational fluid dynamics (CFD) simulations were run to assist the design of both the wind tunnel and the FWC prototype. In addition, different FWC assemblies were tested under real conditions both at the experimental site in Taborno (Tenerife) and in El Pinillo (Gran Canaria).

5. The conceptual idea

Basically, traditional fog water collectors consist of a rectangular standing frame covered with a commercial mesh which is exposed to the predominant winds. Wind driven fog droplets impact by inertia on the screen filaments, resulting on water films that coalesce and build up to a sufficient volume that triggers slipping and drainage by gravity to a reservoir below. Such conventional devices are inefficient, i.e., less than 10% of the liquid water present in the air is recovered. Clogging of the cross-linked screen and re-entrainment of captured water drops back into the wind stream are responsible for such low aerodynamical efficiency. Also, due to their 2D geometry, they are structurally unstable under strong winds. In this respect there has been little innovation so far, principally because the improvement of conventional collectors has been subjected to the availability of inefficient commercial meshes not intended originally for this purpose. With this in mind, the conceptual idea to be tested starts with the virtual sectioning of a flat screen that is displaced on the horizontal axis in a ladder-like structure as schematically shown in Fig. 1. The wind exposed area remains unaltered but, by displacing the original vertical flat collector on the horizontal axis, we gain structural stability. A three-dimensional design is also preferred over 2D geometries, since the former is favourably oriented to the wind most of the time, so water yields would be more stable throughout the year. A 3D structure also favours self-ground-sustenance. In addition, harp-like screens with parallel fibres will be selected instead of cross-linked meshes, because clogging and poor aerodynamics are thus minimised. Therefore, the usual cross-linked mesh will be replaced by a series of 3D printed vertical comb-like collecting surfaces. Unentangled fibres avoid adhesion of drops at intersecting knots, thus reducing the transit time of the collected water within the system. This facilitates fast removal of attached micro-drops and therefore prevents clogging and re-entrainment. Thus, presumably improving the efficiency.

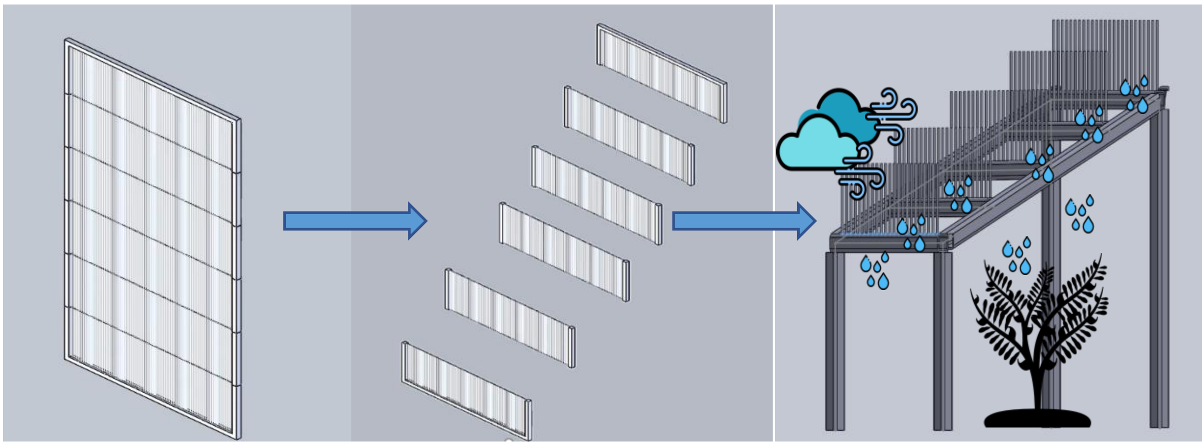

Fig. 1. Conceptual idea behind the prototype design. A traditional 2D flat collector is segmented and projected in a ladder-like arrangement of vertical comb-like screens.

6. Field tests of harp-like screens

Despite the large amount of bibliography generated over more than half a century of fog related studies, little has been advanced on the systematic investigation of fog water collection under natural field conditions. In fact, much of our current knowledge comes from findings obtained from simplified systems of droplet impingement on cylinders and transport of aerosols, such as the wind dispersal of pollen and spores. Consequently, little is known about the optimum configuration of fog water collectors under real field conditions. Notice, that in contradistinction to experiments under a controlled set-up, field data takes into account variable liquid water content, droplet distribution and wind velocity, so this permits us to verify whether conclusions derived in the lab under a single parameter modification (e.g. wind velocity) and artificial fog are extendable to a real foggy scenario with wider variability.

6.1. Optimum single-filament diameter

The field testing of screens at the experimental site in Taborno (Tenerife) was carried out following a bottom-up strategy in terms of complexity. First, we looked for an optimum filament diameter by displaying single nylon wires of variable section, from 0.12 up to 4 mm, under foggy conditions and measuring the fog water collected in plastic bottles below each string (Fig. 2). To this regard, concomitant measurements of meteorological conditions, visibility and fog water collection with a cylindrical fog water catcher, provided us with valuable information. Continuous maintenance of these facilities was necessary. Collected water was measured every two weeks by weighting the filled bottles that were replaced by new ones. Once a sufficiently large data set was gathered, this was filtered based on visibility conditions and concomitant meteorological information provided by the available *in situ* instrumentation. In addition, experiments were also carried out with metal, braided and sanded (with sandpaper of different numbers) filaments to study the effect of microtexture, rugosity and material on the collection efficiency, but no conclusive results were obtained in this respect.

Fig. 2. Set-up of single nylon filaments of varying diameter (top) and detail of collecting bottles (bottom) displayed in the Taborno field site.

Analysis of 3 months of collected data showed that, under variable field foggy conditions, in the long term, the smaller the strand diameter the higher the collection rate per surface unit, i.e. the fog water collection efficiency increases rapidly as the impacting filament section is reduced, in concordance with theoretical results. However, some deviation was observed from previous impaction models encountered in the bibliography (Fig. 3). This behaviour may be explained in terms of the object stopping distance such that, as the filament diameter increases, the air streamlines move around it a greater distance ahead. Consequently, the probability of inertial impaction of fog droplets transported by the wind decreases, since this would scape more easily. The results show that this effect prevails and exhibits a monotonic consistent trend independently of the variability in wind and droplet distribution occurring during the measurement period. This is an encouraging result, that permits us to extrapolate conclusions obtained in the lab to real field conditions with confidence.

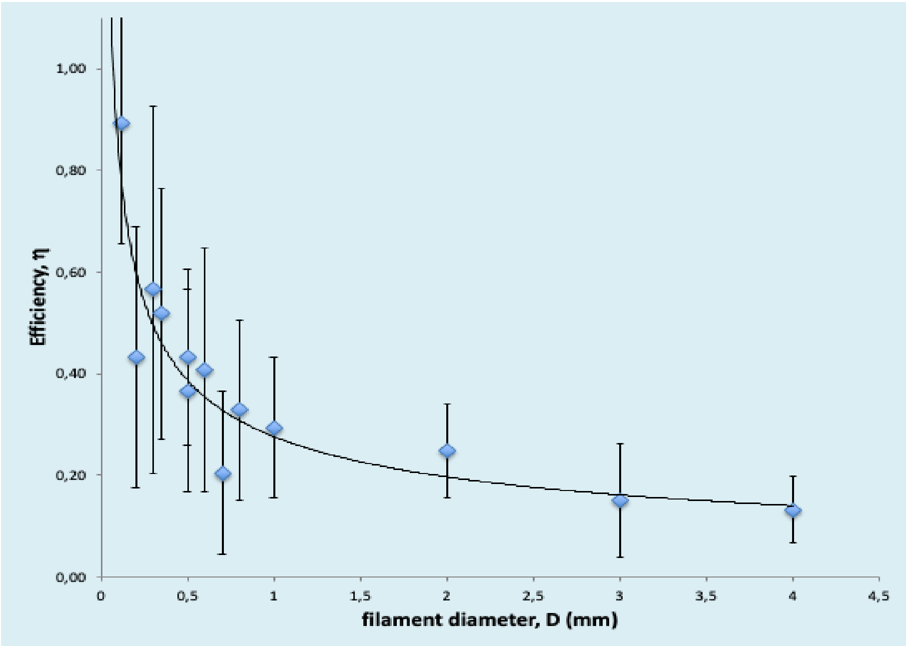

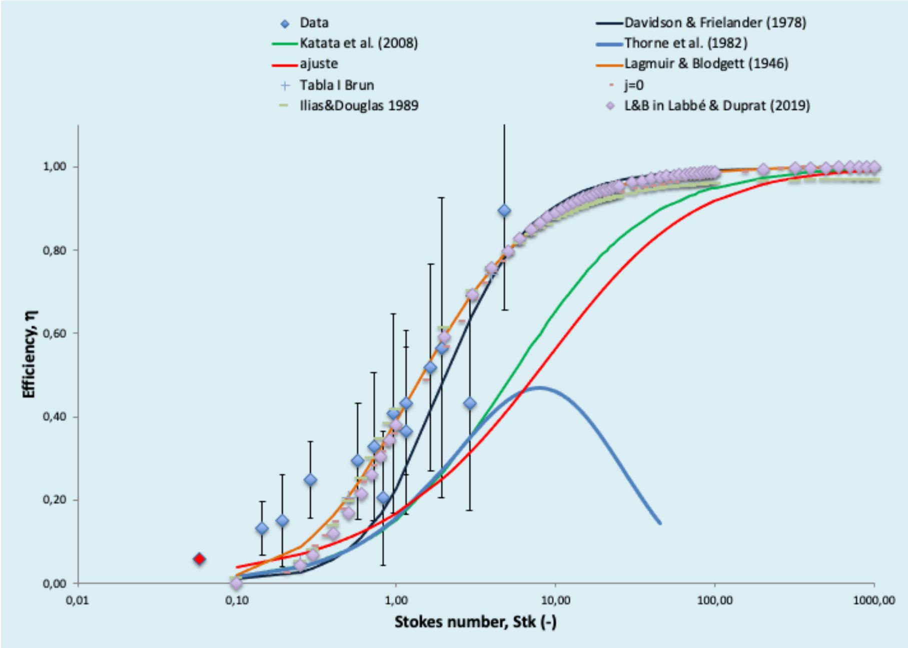

Fig. 3. Dependence of fog water collection with filament diameter (top) under field conditions and comparison with previous fitting impaction models published in the bibliography.

6.2. Aerodynamic effects on the filament interspacing in a harp-like arrangement

In isolated single filament experiments, aerodynamic effects may be disregarded and collection efficiency is mainly affected by the droplet impaction phenomena, as we have discussed above. However, when several filaments are combined in an array, aerodynamic phenomena come into play and, therefore, filament interspacing distance and the shading coefficient of the screen have a relevant effect. In order to study this contribution to the fog water collection yield, we first varied the strand diameter from ∅=0.3, 0.6, 2.4 up to 4 mm, but maintaining a constant fractional coverage of 30% in different 2D harp-like 1 m tall screen displays, i.e. the interspacing was varied from 1 to 13.3 mm (and the number of filaments accordingly). Notice that, in this case, an interplay arises between filament diameter (the smaller the diameter the greater the impaction efficiency) and the number of strings (the thinner the higher the number of filaments and the shorter the interspacing). The different arrangements were initially associated to collecting plastic bottles and then to autonomous individual pluviometers to have a better control over single fog episodes (Fig. 4).

Fig. 4. Experimental set up of harp-like filament arrangements of varying diameter and constant shading coefficient, SC=30% displayed in Taborno experimental site.

The results obtained showed a large variability in the water collection yield during the period of measurement (over 3 months) due to the prevailing meteorological conditions of different fog episodes. In the long term, the cumulative totals revealed to be higher for both the thinner (∅=0.3 mm) and thicker (∅=4 mm) filaments, i.e. closely spaced (1 mm) more efficient thin strings (∅=0.3 mm) collected similar amounts of fog water than thicker (∅=4 mm) widely separated (13.3 mm) filaments of equal overall shading coefficient (30%). Intermediate arrangements (∅=0.6 mm and ∅=2.4 mm) rendered lower yields (Fig. 5). This put in evidence the aerodynamic effects arising as a consequence of the air stream crossing an array of parallel strings and their non-linear contribution over the droplet impaction phenomena on single filaments.

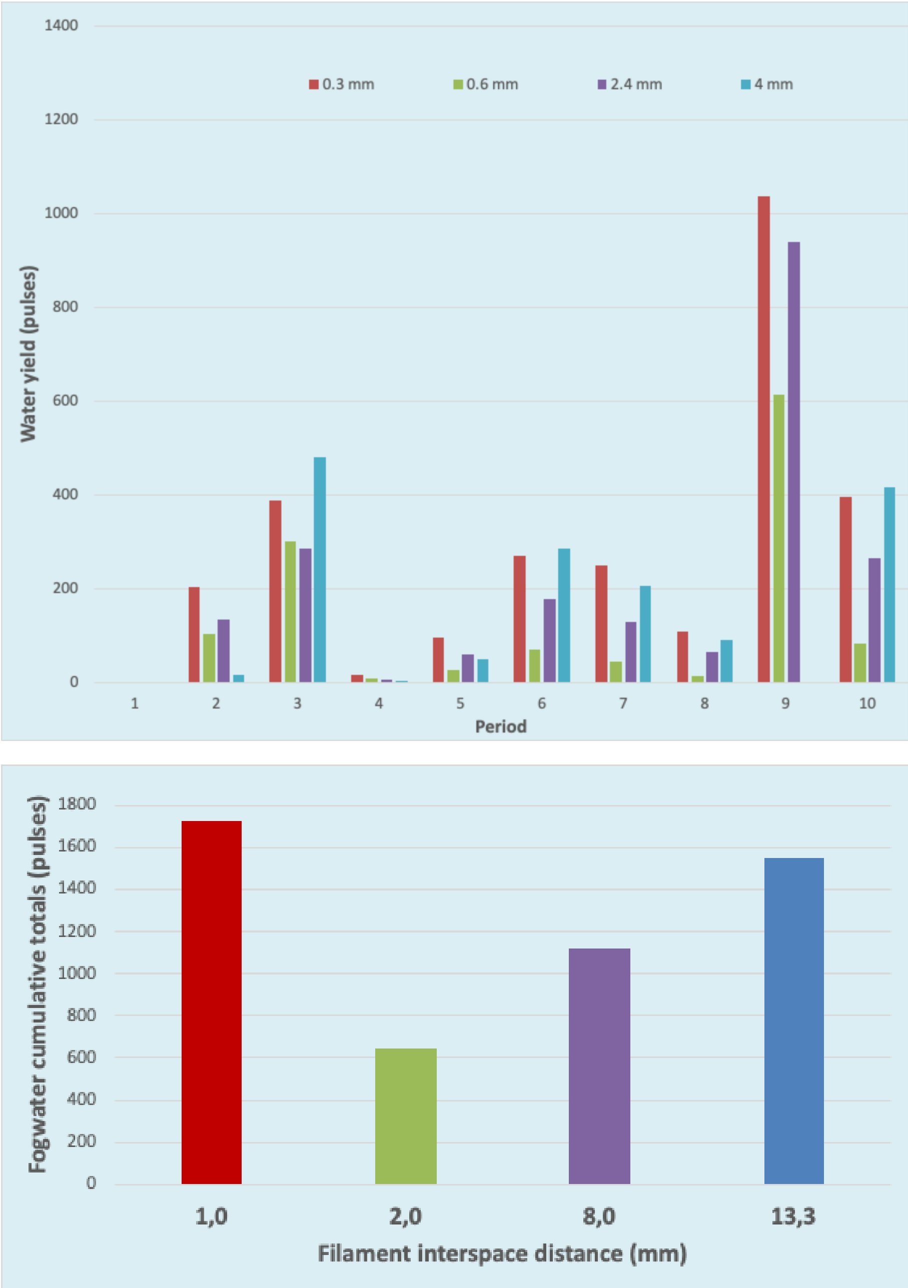

Fig. 5. Fog water collection yields obtained for varying filament interspacing in a harp-like arrangement with constant shading coefficient, SC=30%. Top: variability observed during various foggy periods for the different string arrangements; bottom: variation of total cumulative fog water yield with the filament interspace distance. Each colour corresponds to different filament diameter and interspacing.

6.3. The effect of screen coverage of harp-like arrangements

Finally, we selected a fix filament diameter of 2.4 mm and studied the effect of increasing the screen coverage, from SC=20, 30, 40, 60, up to SC=80%, of different harp 1-m long fog water collectors. The fog water collected was directed to individual pluviometers below connected to a datalogger to have continuous registration of the volumes measured (Fig. 6).

Fig. 6. Experimental set up of harp-like filament arrangements with different shading coefficient (from left to right: SC= 30, 20, 40, 60, 80%) displayed in the Taborno experimental site.

A fractional coverage of 30% provided maximum cumulative collection yields, i.e. neither the tightest mesh (SC=20%) nor the most open (SC=80%), but an intermediate covered screen (SC=30%), was the one that collected more fog water (Fig. 7). This shows the need of considering not only the droplet impaction phenomenology (i.e. single filaments) but, more importantly, the aerodynamic effects emanating from the 2D arrangement of filaments. In the next step we aim to combine the best of both worlds, i.e. maximum coverage with increased aerodynamic efficiency, by fabricating 3D multiple layer staggered meshes and systematically testing them in the wind tunnel.

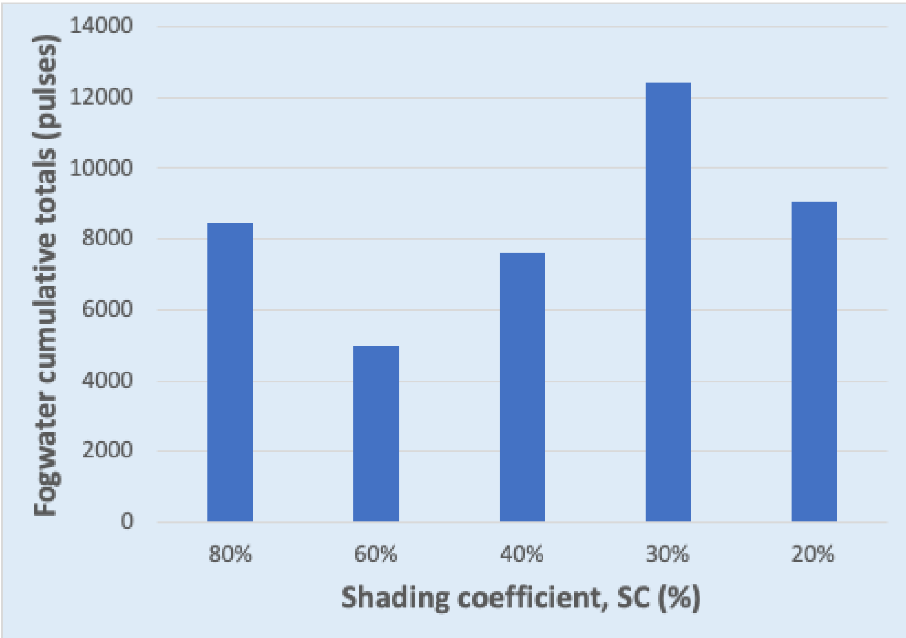

Fig. 7. Variation of total cumulative fog water yield under field conditions of harp-like filament arrangements of varying shading coefficient, SC.

7. Instrumentation for the lab experiments

As discussed above, many parameters affect the collection of fog water: diameter, geometry and orientation of the impacting screen elements, shading (i.e., percentage of area covered by the solid screen) and number and disposition of collecting layers. Also, the fog liquid water content, size of droplets and wind velocity are relevant issues to take into account. To be able to keep control of these manifold variables, we built and instrumented a wind tunnel to carry out experiments where each of them are modified sequentially.

6.1. The wind tunnel

The wind tunnel is shown schematically in Fig. 8. To arrive to the definitive design, a series of computer simulations were carried out to confirm the absence of vortices and that laminar flow was achieved along the wind tunnel in collaboration with the University of La Laguna (ULL) (Fig. 9). Also, the geometry of its different parts was optimised by means of numerical experiments to ensure the right conditions in pressure drop, air velocity gradients and attachment of the boundary layer necessary for the correct mixing of the artificial fog atomized inside the tunnel. Once we were confident that these conditions were met, we proceed to the construction. Fig. 10 shows different stages during the assembly of the tunnel at the ICIA mechanical workshop and the resulting finalised structure located in the hydraulic lab. From left to right, the 6 m long tunnel consists of a 3 m galvanized steel sheet diffusing cone where the fog water nebulizers are introduced through different orifices on the side (see below); this is attached to a contraction cone prior to the removable methacrylate test chamber, where the fog collector prototypes are inserted; it follows a diffuser and an electric fan to circulate the air along the tunnel. A variable frequency drive (AFD) permits control of the fan velocity and therefore a range of wind speeds from 2-8 m s^{-1}, typical under field conditions (Fig. 11). Wind velocity and relative humidity inside the tunnel during the experiments were monitored with a hot-wire anemometer (Beha Amprobe) (Fig. 12). The pressure drop ahead the tested fog water collection screens was measured with a Pitot tube (PCE Instruments) (Fig. 13).

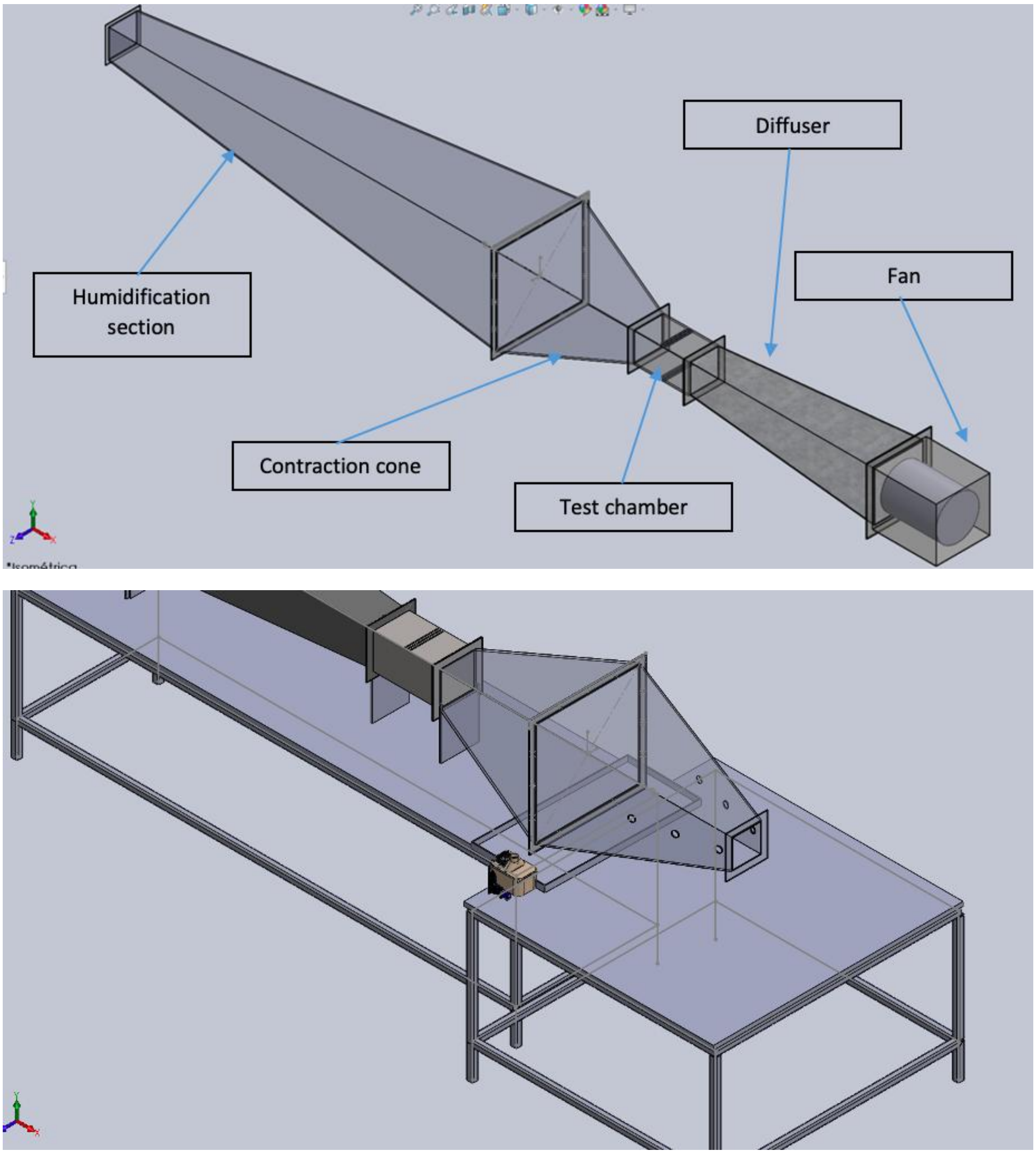

Fig. 8. Scheme of the wind tunnel showing its different parts.

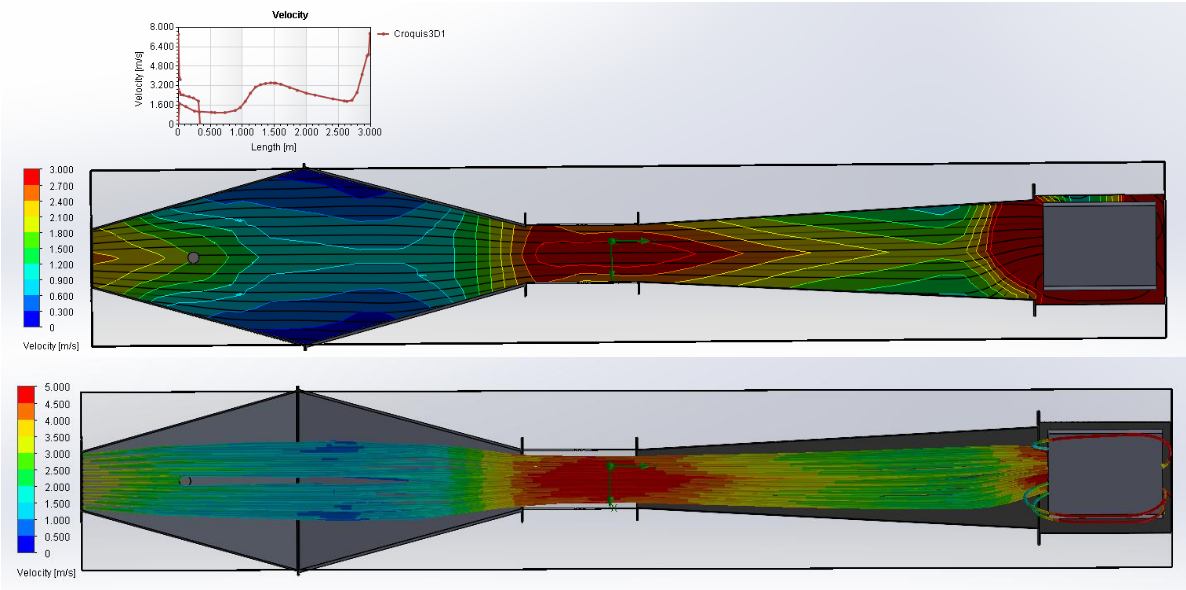

Fig. 9. An example of the series of prior computer simulations carried out for the correct design of the wind tunnel.

Fig. 10. Different stages during the construction of the wind tunnel by ICIA personnel and the final product located in our hydraulic lab.

Fig. 11. Fan and variable frequency drive (AFD) for controlling the air velocity inside the wind tunnel.

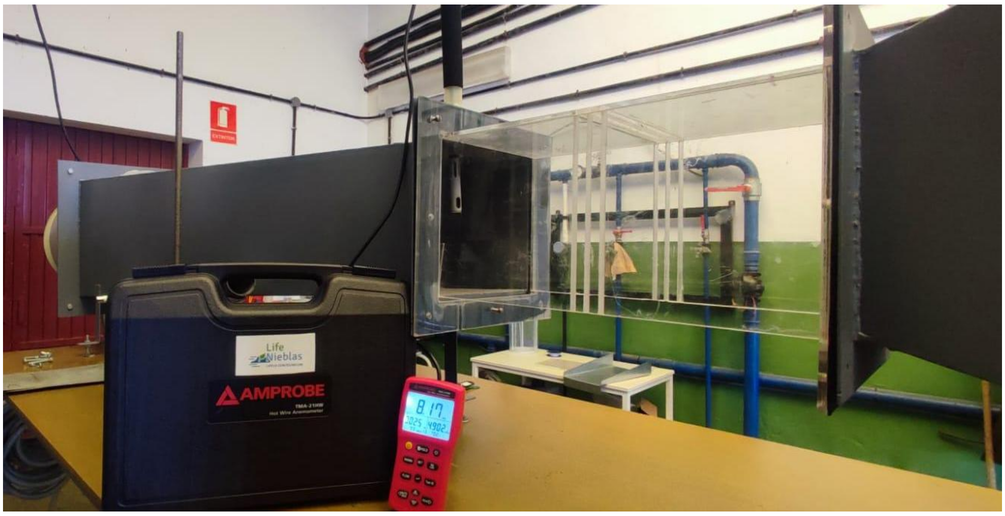

Fig. 12. Handheld and hot-wire anemometer for monitoring air velocity and relative humidity inside the wind tunnel.

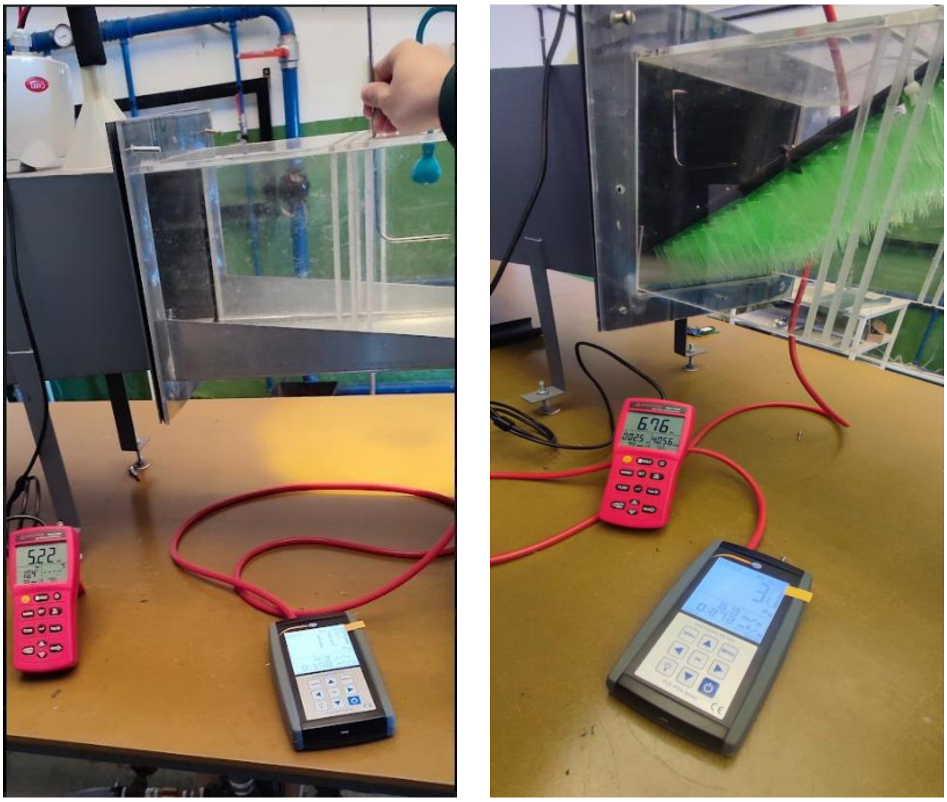

Fig. 13. Handheld and Pitot tube air flow meter for measuring pressure drops inside the test chamber as a consequence of interruption of the wind stream by the fog water collection prototypes tested.

6.2. Instrumentation of the wind tunnel: artificial fog water droplet generation

In order to reproduce the characteristics of the real fog present in the field, high relative humidity (>95%) and a range of water micro-droplet sizes (1-50 µm) are needed. Thus, different humidification systems were introduced along the diffusing cone to meet these requirements (Fig. 14). First, on the wind tunnel entrance, an adiabatic humidifier increases the relative humidity (RH) and lowers the temperature of the ambient air by spraying water on a bank of screens. Next a steam humidifier further increases the air water vapor content up to values of RH> 95% inside the diffuser. After revising the available literature and possible suppliers, two different fog generating systems were selected This was so in order to cover the whole span of droplet sizes present in natural fog (1-50 µm). An ultrasonic nebulizer, that produces small drops in the lower range (1-5 µm), and also a high-pressure nebulizer for the upper droplet diameter interval (5-50 µm) were acquired. For the former we chose the Humisonic nebulizer and for the latter the adiabatic atomizer ChillBooster from Carel Industries. The Humisonic consists of a small water storage tank and piezoelectric transducers that vibrates in order to produce the vapour mist. The ChillBooster essentially comprises a cabinet with a 10 bar pressurizing pump and a system of nozzles mounted onto steel manifolds to be arranged around the condensing unit (Fig. 15). To meet the water pressure requirements of this equipment, a pumping and filter system was installed prior to the inlet of the Humisonic and the Chilbooster (Fig. 16). Leftover water was derived to a tank and recirculated to minimize water waste (Fig. 17). Fog water collection efficiencies and yields of the prototypes were calculated from the weight difference between the consumed and drained water below the screen measured with two balances (Fig. 18). These were connected to a computer such that weights could be registered continuously (Fig. 15).

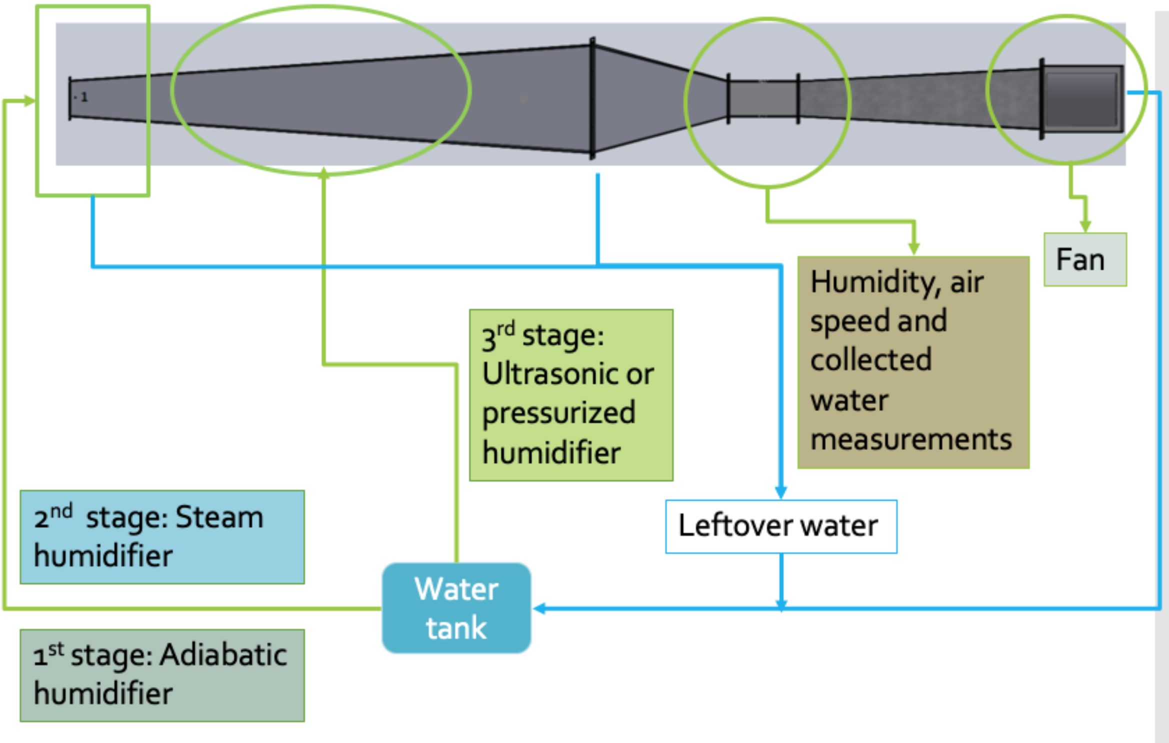

Fig. 14. Different stages of the artificial fog conditions generated inside the wind tunnel.

Fig. 15. From top to bottom: Ultrasonic fog generator, steam humidifier, high pressure atomizer, duct distributor with spraying nozzles and overall view of the instrumented humification cone of the wind tunnel.

Fig. 16. Water pump system installed at the inlet of the ultrasonic humidifier.

Fig. 17. Recirculation system showing water pump and storage tank.

Fig. 18. Digital balance at the Humisonic inlet (left) and at the wet chamber drainage gutter (right) to measure weighing differences for determination of fog water collection yields of the prototypes.

6.3. Instrumentation of the wind tunnel: water vapour phase generation

During the course of the early experiments in the wind tunnel we detected that variations in the ambient temperature and relative humidity (RH) conditions were affecting the results. Low humidity provokes evaporation of the injected fog microdroplets and therefore fog water collection may be hindered. Thus, in order to achieve a higher and more stable RH, an adiabatic humidifier was designed and constructed at ICIA mechanical workshop. This is comprised of a cube with a series of parallel vertical screens placed inside, where water is sprayed by means of micro sprinklers (Fig. 19). A tray below collects the dripping water and this is recirculated with a pump. The system works under the principle of adiabatic cooling whereby a wet surface evaporates and therefore decreases its temperature. As the air passes through the wet screens this increases the RH and reduces its temperature. By placing the adiabatic humidifier at the entrance of the wind tunnel, higher and more stable humidity of the air stream was therefore achieved.

Fig. 19. Adiabatic humidifier constructed at ICIA placed at the entrance of the wind tunnel. In the right hand side photo, the shading screens have been removed to show the sprinkling system used to wet and cool the passing air.

About a 10% increment in the RH of the incoming air was attained with the above system. However, in order to reach conditions close to vapor saturation characteristic of the foggy environment in the forest (RH>95%), an active water vapor generator is required. We intend to reproduce natural environmental features as close as possible, such that results now obtained in the lab may be extrapolated later to the field with confidence. Thus, a steam humidifier, not initially planned in the project instrumentation, was acquired. After some calculations of the steam flow rate needed for a range of air velocities of 2-8 m s^{-1} inside the wind tunnel, we decided to buy the heaterSteam UR002 (Carel Industries, S.p.A.) which can provide up to 2 Kg h^{-1} of water vapor and reach RH=100% with a precision of ±1% (Fig. 20).

Fig. 20. Steam humidifier acquired to be able to reproduce inside the wind tunnel foggy conditions close to those present in the field. Close-up view of the heaterSteam (left). Water

vapor flow across the wind tunnel section. The methacrylate test chamber has been removed for better visualization of the saturated air stream (right).

6.4. Design and 3D printing of the prototypes

The different prototypes were digitally sketched with the help of a design software (Fig. 21) and manufactured with a resin-based 3D printer (Fig. 22). Such an additive technique enabled us to rapidly produce models with different shapes, filament length and geometries, interspacing, etc. These were then tested in the wind tunnel in order to optimise their fog water collection capabilities.

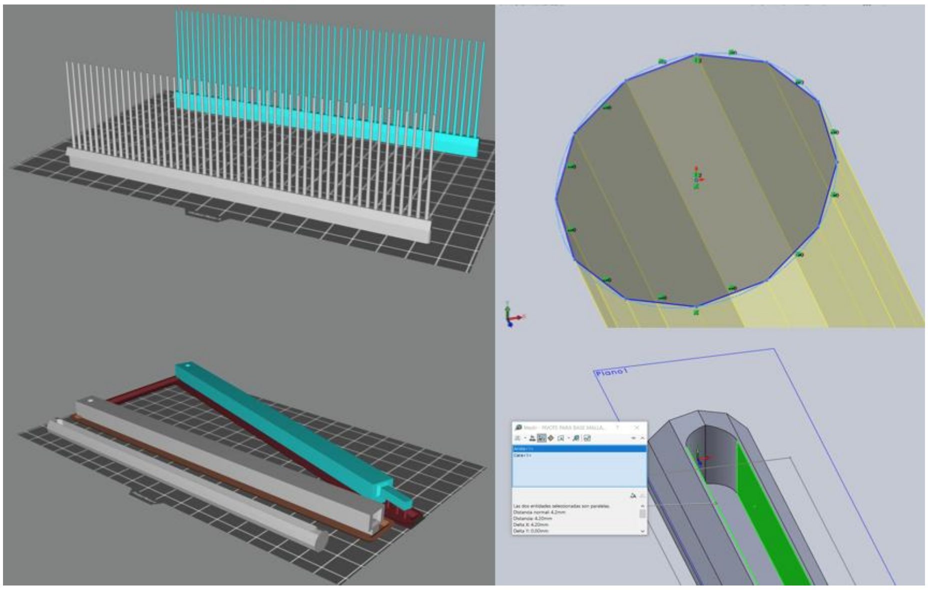

Fig. 21. An illustration of the process followed during the graphic design of the different parts of the prototypes devised.

Fig. 22. 3D printer (left) and drying chamber of the resin printed models (right).

8. Characterization of commercial screens

As a starting point, we first characterised different commercial meshes in order to gather information about available screens and their design parameters: size of filaments, shading, geometry of interspaces, etc. (Table 1).

Mesh type	Opening geometry	SC (%)	Width (mm)	Image
Single layer Raschel	Triangular (6x6x6 mm)	26.5	1.25	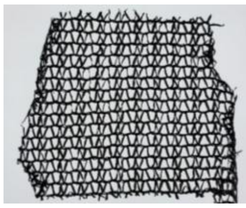
Double layer Raschel	Irregular	78.6	1.25	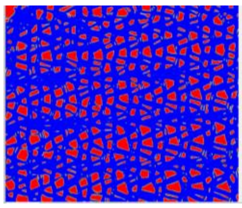

Mosquito net	Squared (1.5x1.5 mm)	29.6	0.25	
Metallic screen	Squared (9x9 mm)	9.1	0.75	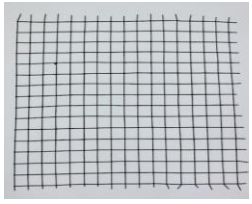
Polymeric screen	Squared (3x3 mm)	28.2	0.3	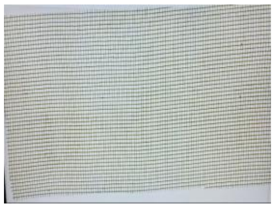

Table 1. Some commercial meshes characterised and their design parameters: geometry and dimensions of opening interspaces, shading coefficient (SC), and filament width.

Screens were scanned and the resulting digital images were processed in order to quantify these parameters (Fig. 23). One of the inconveniences detected for some commercial screens is the low reproducibility of their design parameters. Therefore, we also 3D printed (e.g. Raschel mesh, Fig. 24) or constructed (harp-like, Fig. 25 left) some analogues of the commercial counterpart to have a better control over their behaviour. Some of them were tested in the wind tunnel. Although these assays were not systematic, this gave us the opportunity of both operating the wind tunnel with some real material and become familiar with this type of experiments, but also to evaluate the water collection behaviour of commercial screens and their limitations, such as low efficiency, clogging, re-entrainment, etc. (Fig. 25). We next move to design and test a FWC in order to resolve some of these limitations and others of traditional collectors already commented above. This is detailed in next section.

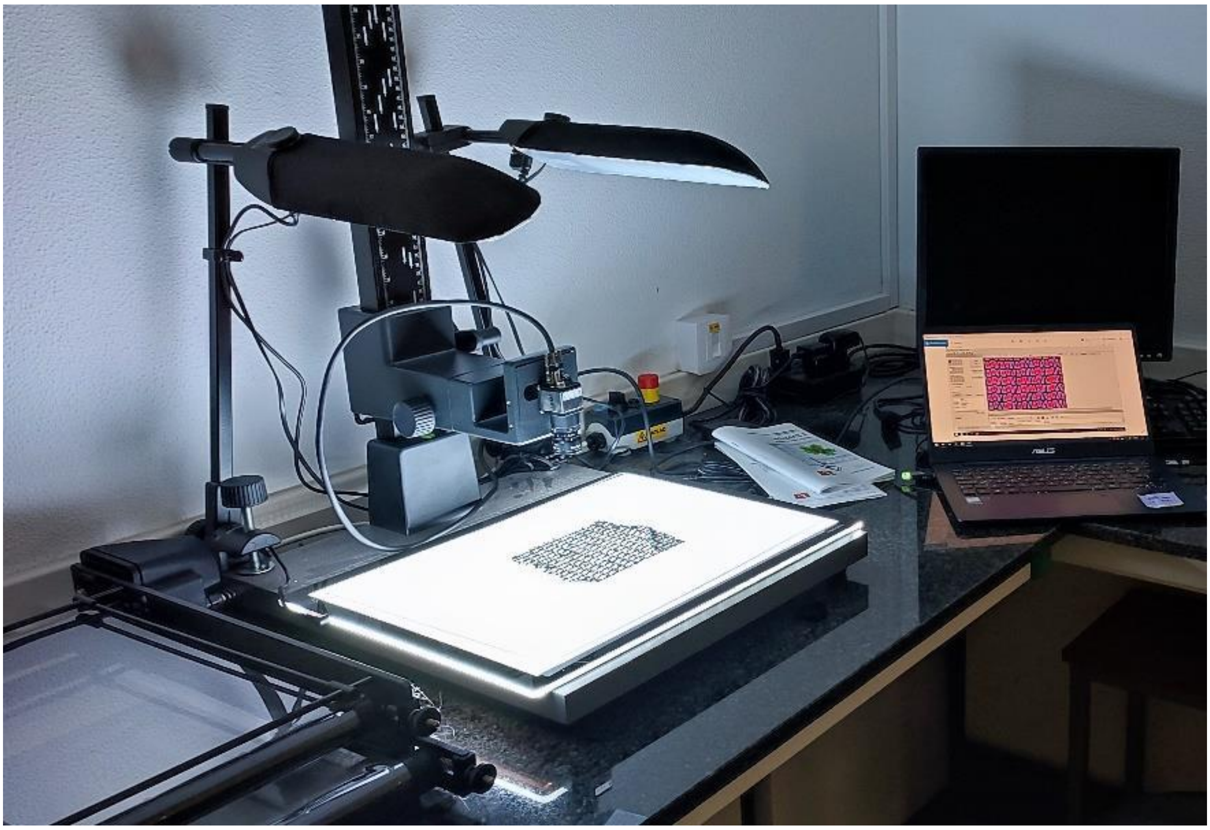

Fig. 23. Scanning of a single-layer Raschel mesh and its digital processing.

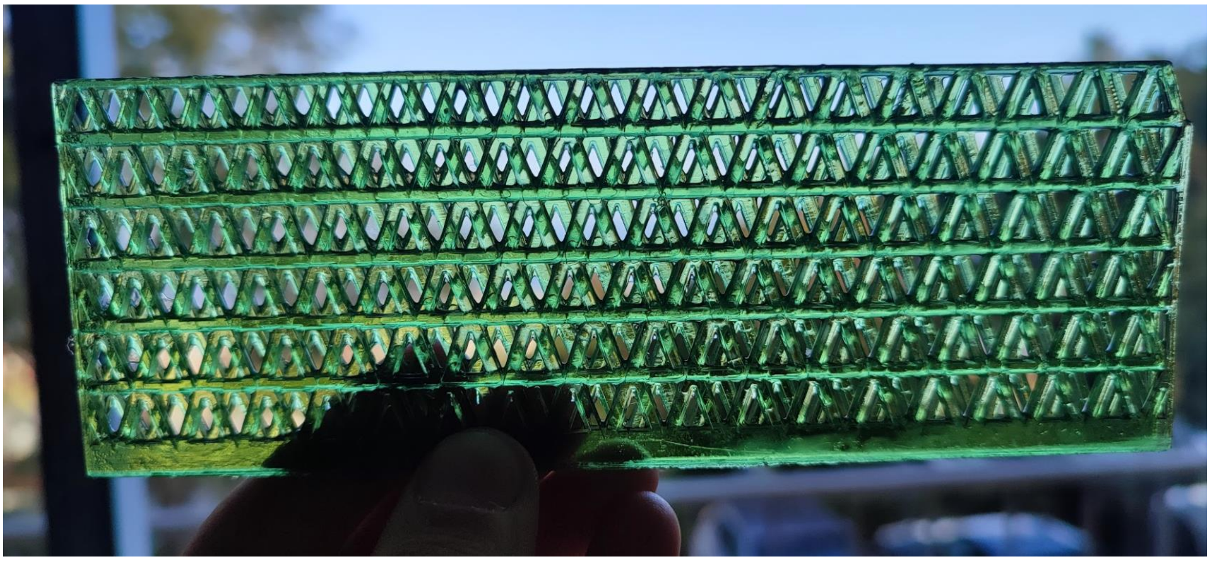

Fig. 24. A 3D printed analogue of a double layer Raschel mesh.

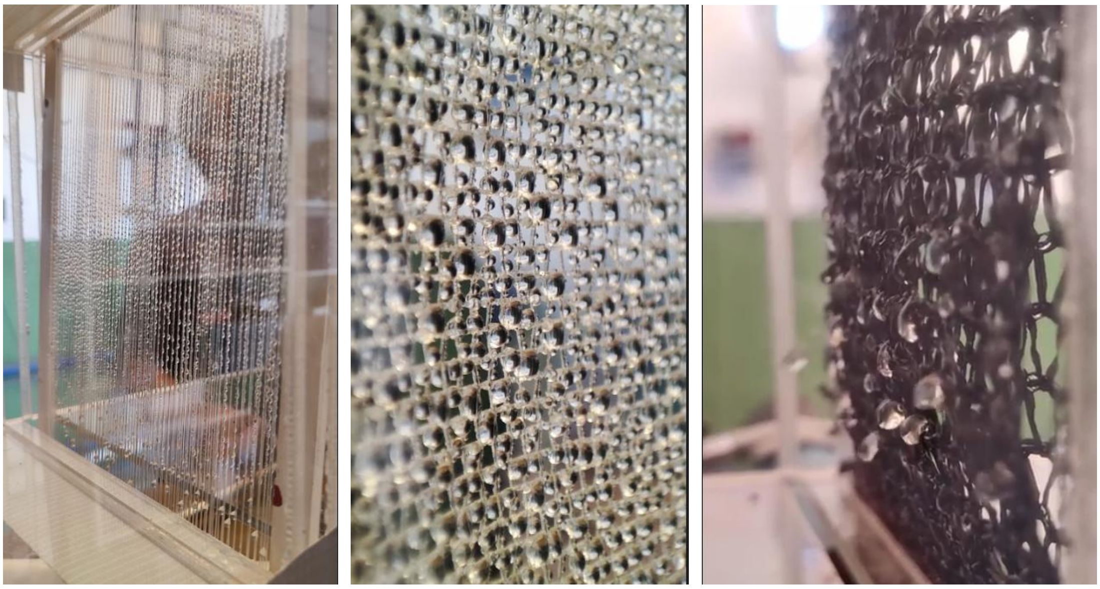

Fig. 25. An illustration of commercial screens fog water collection behaviour in the wind tunnel and their limitations, such as (from left to right) reduced efficiency due to low shading coefficient, clogging, and drop re-entrainment back into the wind flow.

9. Results obtained with the different 3D-printed FWC designs tested in the wind tunnel

In order to optimize the proposed fog water collector, we need to investigate different parameters that affect the collection of fog water droplets. Length, diameter, geometry, angle of inclination, inter-spacing, hydrophilicity and surface microtexture of filaments; number and distance between either in-line or staggered rows; slope and shape of the whole assembly are the main characteristics that may affect both the impaction and aerodynamical efficiencies. We decided to act upon physical and not chemical features of the construction material of the screen because of its final field destination, where it will be subjected to external harsh conditions that could affect any surface chemical treatment of the filaments. For this purpose, we 3D printed an adaptable structure where to easily carry out sequential changes to the configuration of the devised prototypes (Fig. 26).

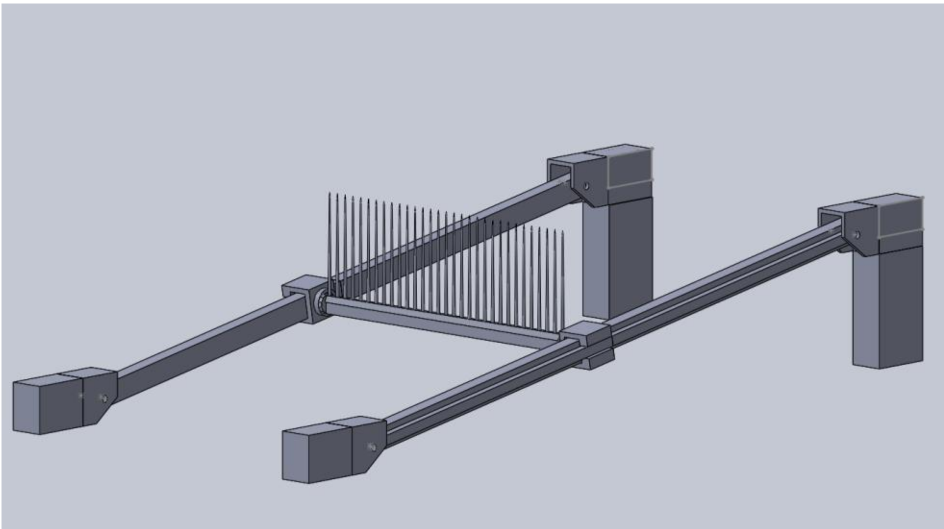

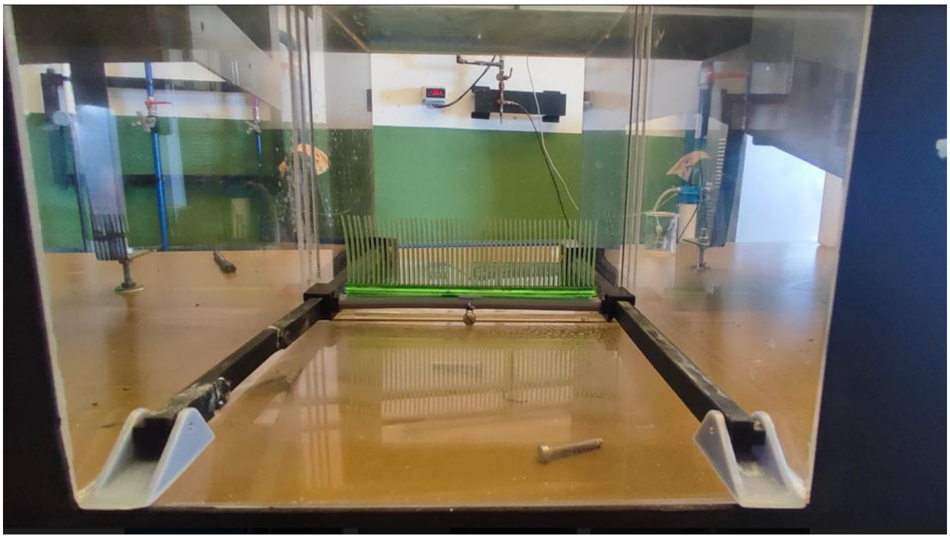

Fig. 26. Versatile structure designed to accommodate the different prototypes to be tested inside the wind tunnel by varying the inclination of the 3D printed screens, number of rows, slope, wind attack-angle, etc. Top: original graphical design; bottom: final 3D printed structure inside the wind tunnel test-chamber.

8.1. Length, diameter, and geometry of the screen filaments

We tested different diameters, lengths, and geometries of single filaments in order to maximize their fog water collection ability. Also, their surface microstructure was investigated. Both, theoretical models and our previous field experiments, indicate that the smaller the filament's diameter the higher its collection rate. This is a direct consequence of the way fog droplets are collected by inertial impaction. An increase in the radius of the filament causes the air streamlines to bifurcate around the obstacle a larger distance ahead and therefore the probability of droplets scaping from inertial impingement increases. However, the size (diameter and length) of the filaments is constrained both by the 3D printing technique available and by their resistance to breakage. Thus, a compromise was achieved between durability and collection efficiency in a series of trial-and-error experiments, facilitated by the 3D printing technique adopted, that permitted fast manufacturing of different prototypes *ad hoc* (Figs. 27-28; Appendix I). In addition, the filaments geometry is important for both impaction and aerodynamic efficiency but also structural compliance. After a series of tests in the wind tunnel, we arrived to a compromise of all these parameters. We finally selected 5-cm-long conical cylinders (0.6° conicity), 1.5 mm diameter at the base ending on an acute pointing tip. The conical shape provides greater stiffness than e.g. cylindrical geometries, but also a variable diameter along the filament that permits capture of microdroplets of different sizes. It is also aerodynamically convenient as the cross-flow air can circulate around the cones smoothly. The strands were oriented pointing downwards, such that differences in the receding and advancing contact angle facilitate the displacement of the pinned drops and evacuation. The acute ending of the conic fibres reduces adhesion of the hanging drops at the tip and thus also facilitates drainage (Fig. 29). In addition, we tested if incorporating microstructure to the filaments surface in the form of longitudinal grooves would facilitate water channelling and evacuation, and therefore would increase the collection rate as it has been suggested in the bibliography (Fig. 30). However, this did not render significant improvements in fog water yield and therefore, for the sake of simplicity, we finally opted for smooth conical fibres. Finally, we also verified whether different cross-sectional geometries of the conical filaments would affect the aerodynamics around them and therefore the fog water collection. We tested square, elliptical and wing-like conical shapes (Fig. 31). No meaningful differences in collected volumes were obtained and therefore we stuck to the original geometry (results not shown).

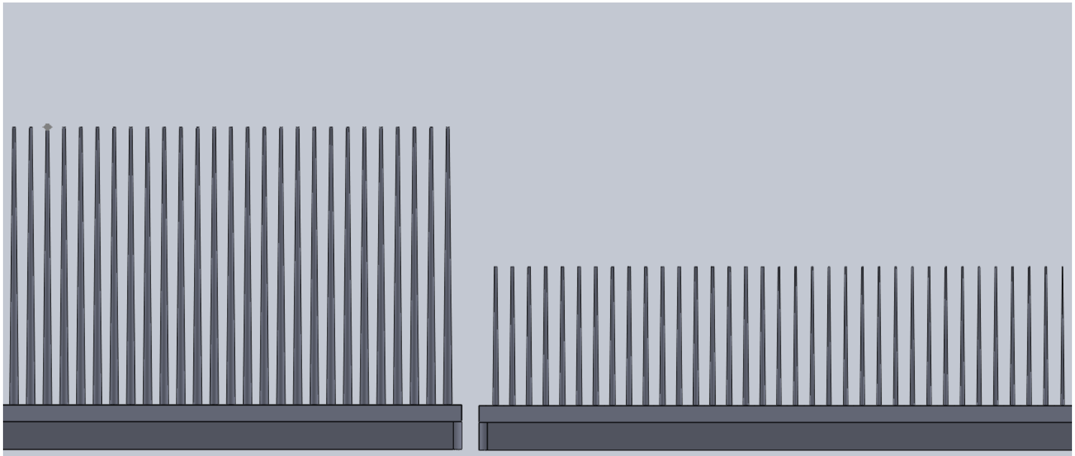

Fig. 27. Comparison of two designed screens with different filament's height, interspace and diameter. These were then 3D printed and tested inside the wind tunnel in order to find an optimum shape and arrangement of the filaments.

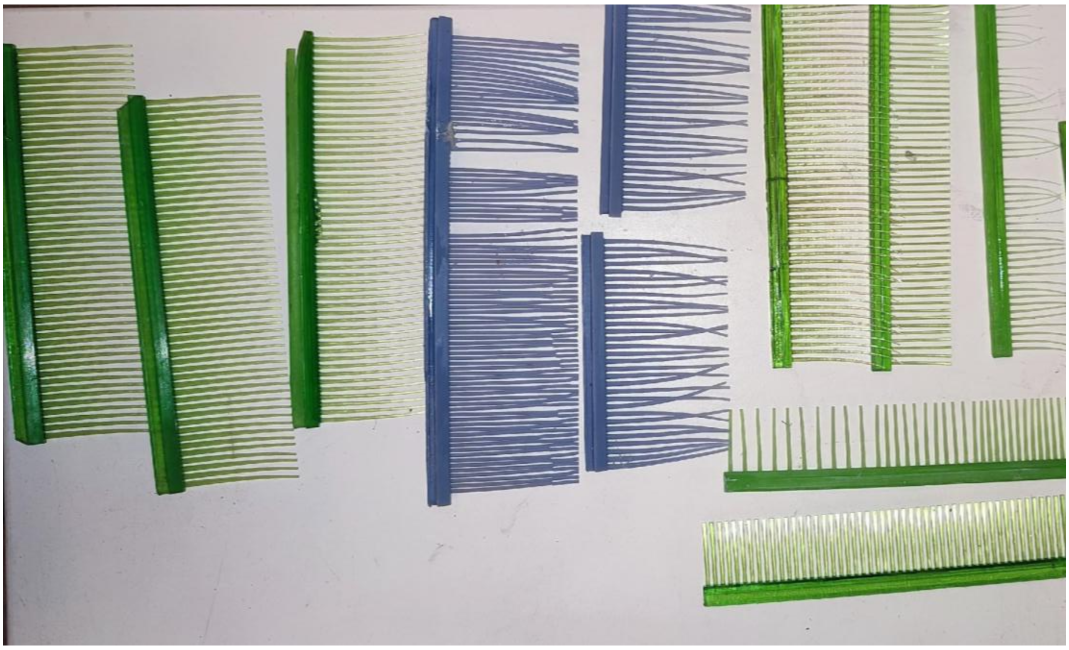

Fig. 28. Some examples of 3D printed screen models manufactured to evaluate the optimum geometrical filament parameters.

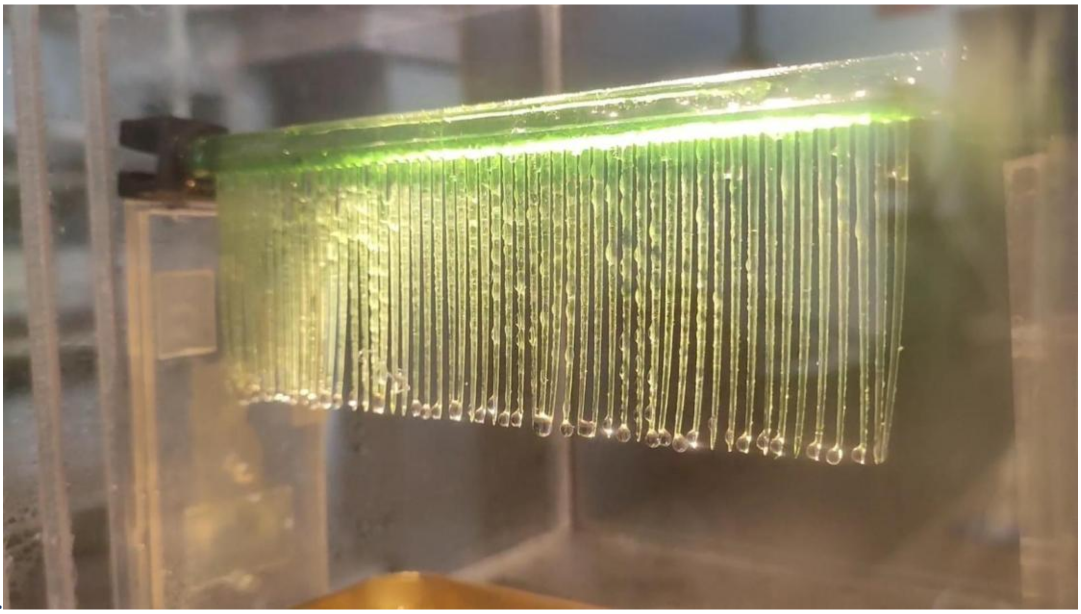

Fig. 29. Close-up view of a 3D printed screen inside the test chamber of the wind tunnel where attached fog water drops can be observed.

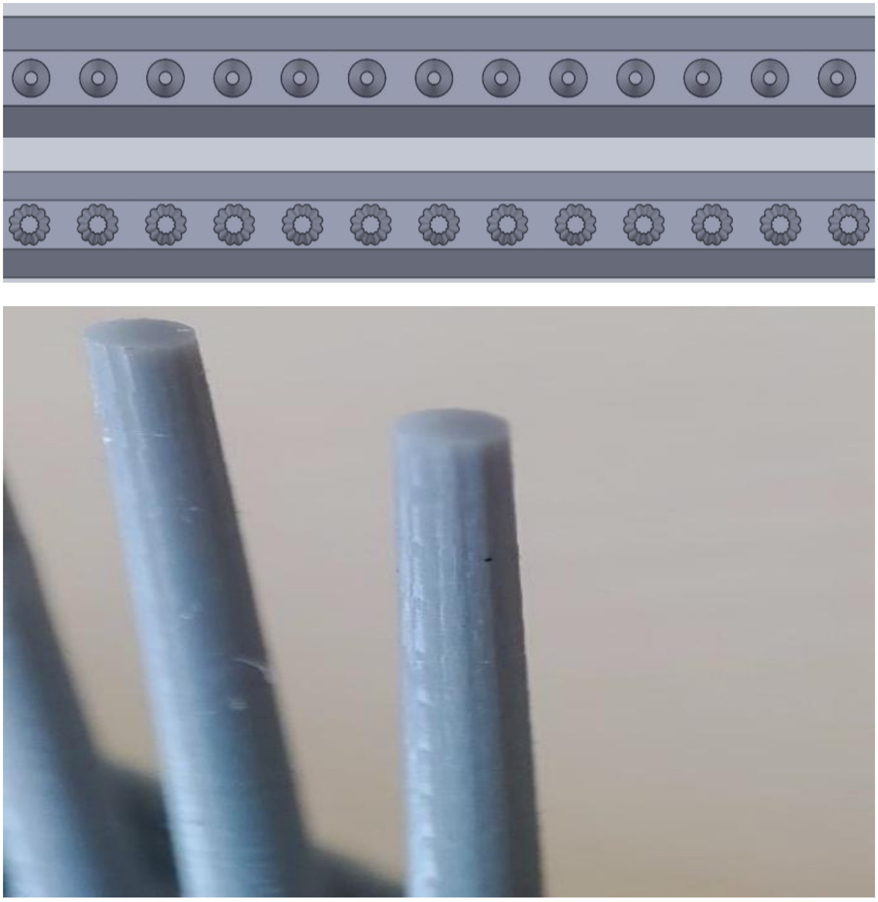

Fig. 30. Upper view of grooved vs. smooth conical filaments designed (top) and 3D printed (bottom) to evaluate the effect of surface microtexture.

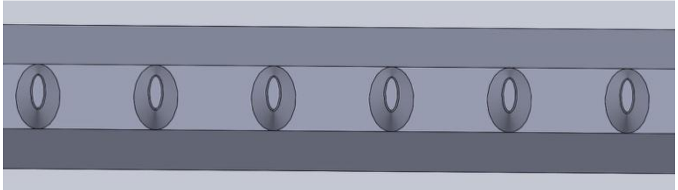

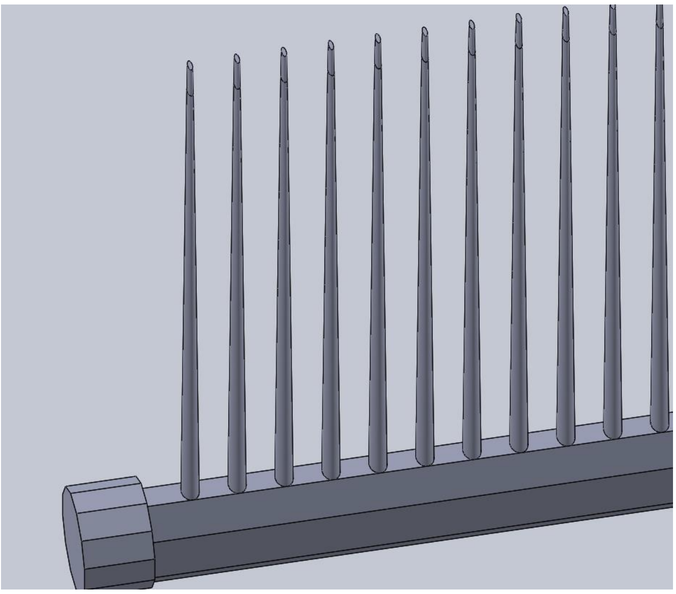

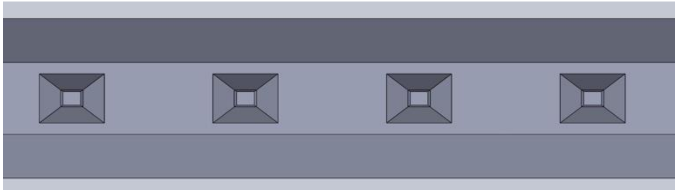

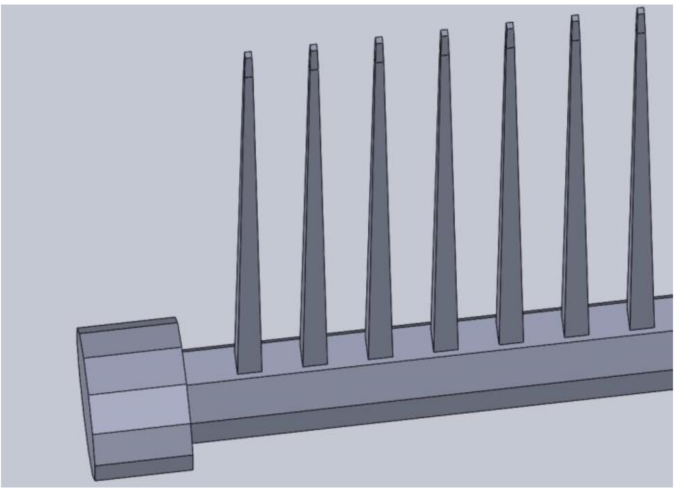

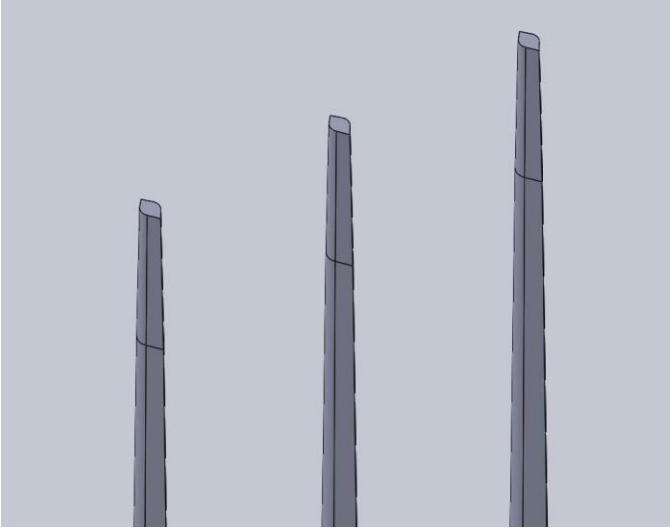

Fig. 31. Images of filaments with different cross-sectional geometries designed to evaluate aerodynamical effects. From top to bottom: elliptical, squared and wing-like.

8.2. Interspacing in a row of filaments

A fog water collector may be visualized as an aerosol filter. The larger the separation distance between threads the lower the capacity of filtration, but a too dense mesh would be obstructed easily and thus would not let the air pass through. Therefore, a compromise between maximising both the impaction efficiency, by increasing the shading coefficient (SC) of the screen, and the aerodynamical efficiency, by reducing the coverage fraction of the conical fibres, must be achieved. Such a "sweet-spot" in SC was found by varying the center-to-center interspacing between filaments from 1.5 up to 8 mm, rendering a shading coefficient from SC=64 down to SC=12 %, respectively, and measuring the collected water volumes in the wind tunnel. A maximum around SC=34.8% (2.7 mm center-to-center spacing) was obtained, i.e., as expected, a rather dense but not too closed lattice was optimal. This maximum is reached at the cross point between the water yield per filament and the number of filaments in a row (Fig. 32). Numerical simulations confirmed that, with such shading coefficient, pressure drops are small and that the air flow crosses the screen with ease (Fig. 33).

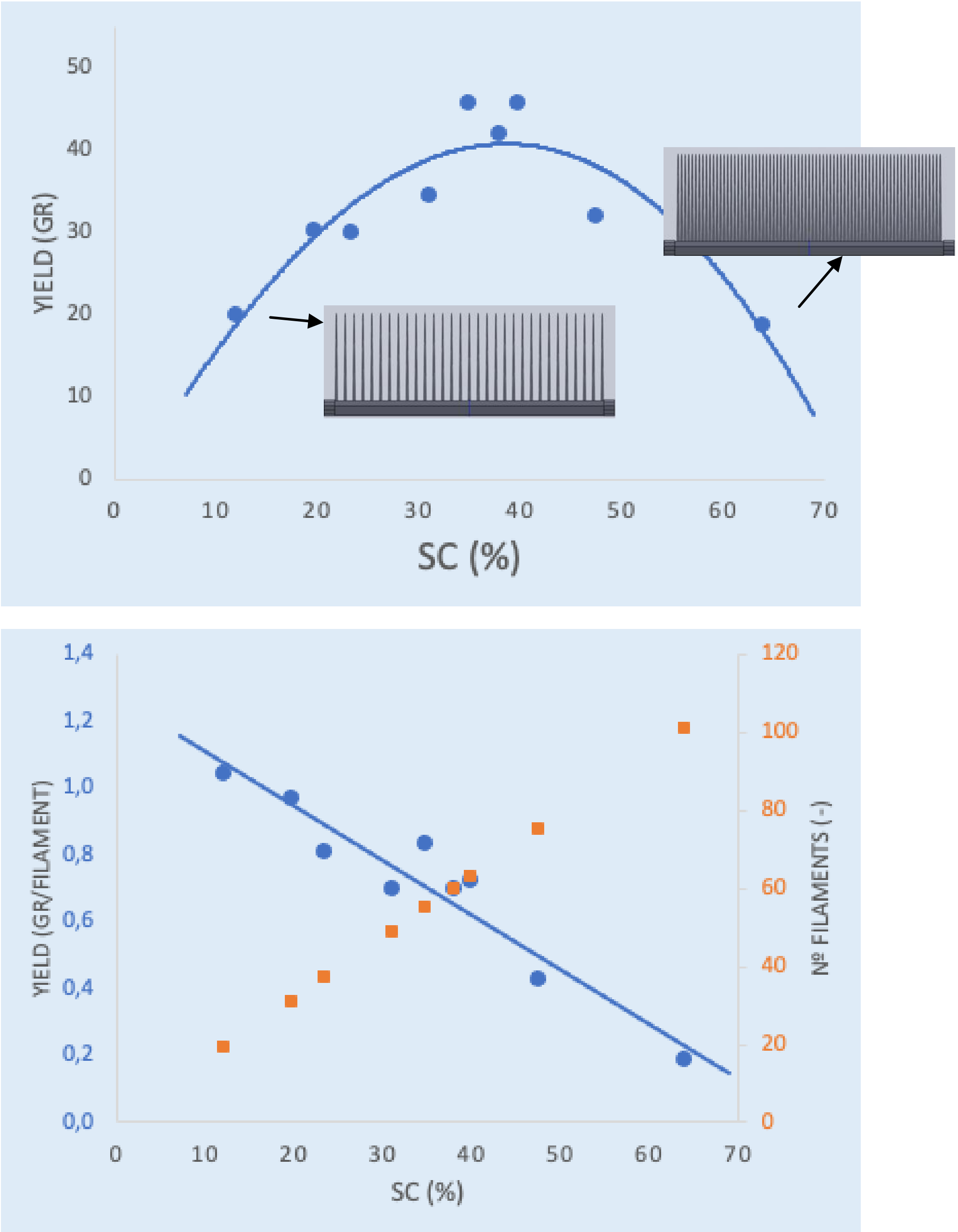

Fig. 32. Variation in the fog water yield as a function of the shading coefficient (SC) from a widely open screen (left) to a closely spaced arrangement of filaments (right). Top: Solid circles correspond to the water collected by fibre assemblies with different interspacing, i.e. SC, and the line is the data fitting curve. Bottom: Yield per filament and number of filaments for different shading coefficients tested.

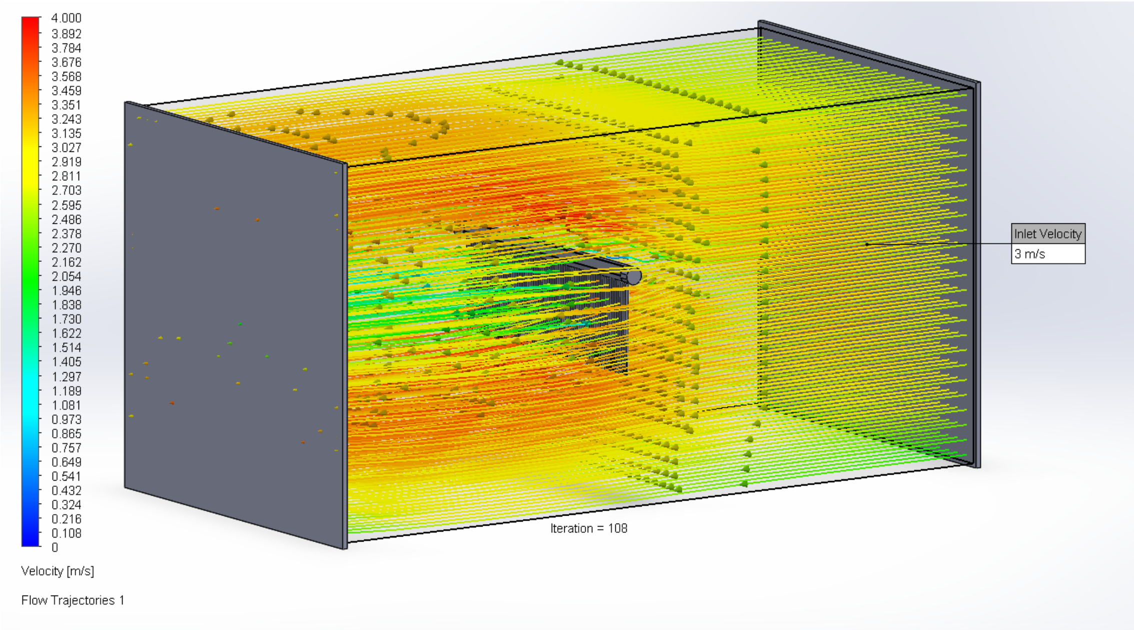
4.000
3.892
3.784
3.676
3.568
3.459
3.351
3.243
3.135
3.027
2.919
2.811
2.703
2.595
2.486
2.378
2.270
2.162
2.054
1.946
1.838
1.730
1.622
1.514
1.405
1.297
1.189
1.081
0.973
0.865
0.757
0.649
0.541
0.432
0.324
0.216
0.108
0
Inlet Velocity
3 m/s
Iteration = 108
Velocity [m/s]
Flow Trajectories 1

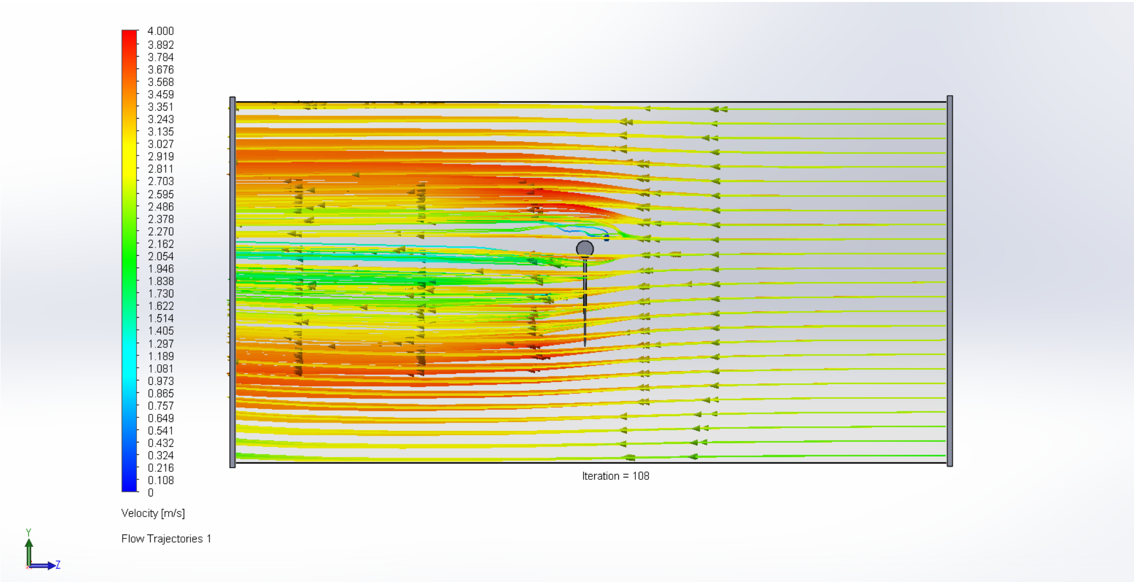
4.000
3.892
3.784
3.676
3.568
3.459
3.351
3.243
3.135
3.027
2.919
2.811
2.703
2.595
2.486
2.378
2.270
2.162
2.054
1.946
1.838
1.730
1.622
1.514
1.405
1.297
1.189
1.081
0.973
0.865
0.757
0.649
0.541
0.432
0.324
0.216
0.108
0
Iteration = 108
Velocity [m/s]
Flow Trajectories 1
Y
Z

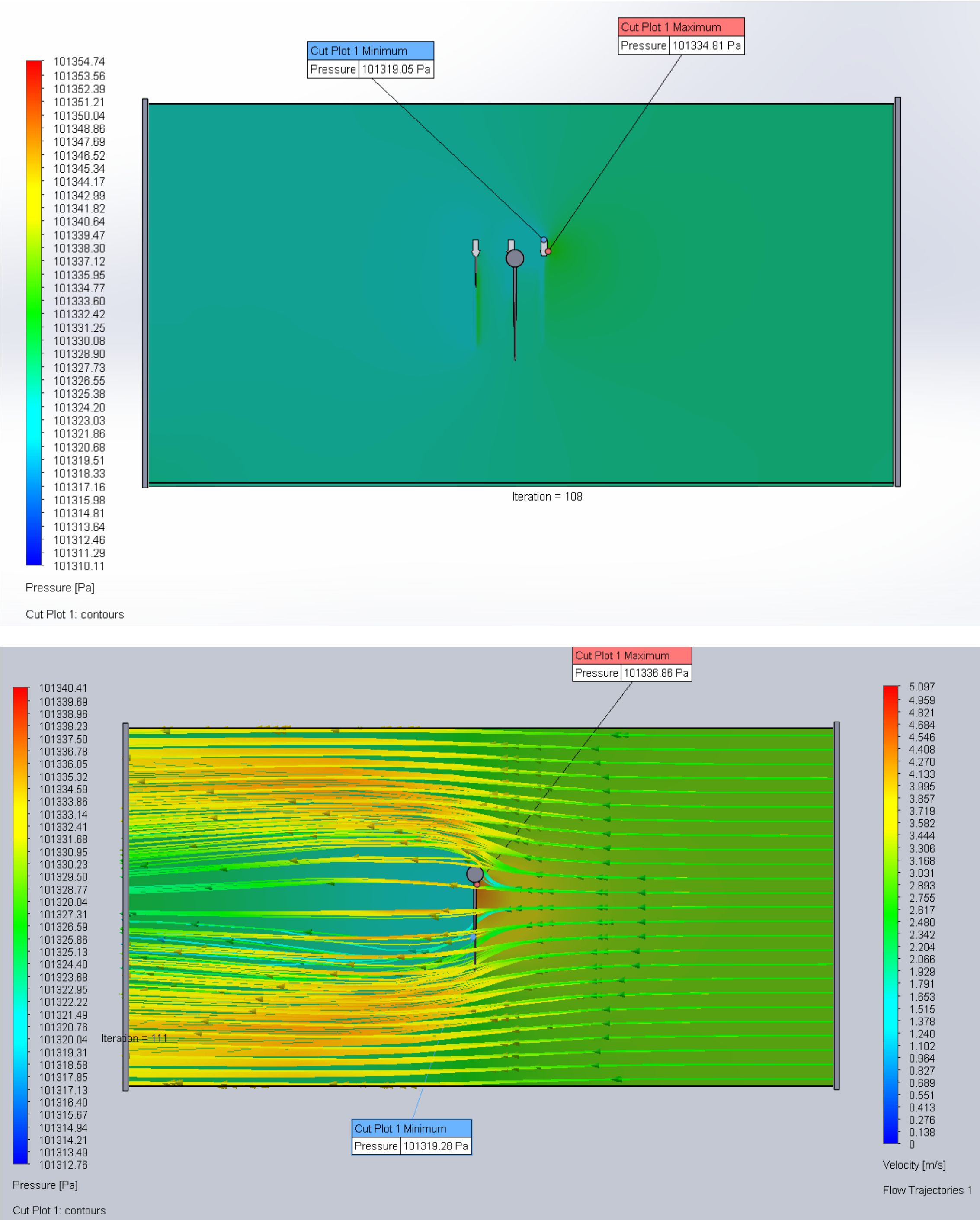

Fig. 33. Numerical simulations of a single layer screen inside the test chamber. Three-dimensional (top) and cross-sectional view of the trajectories, velocity and pressure fields at wind speed of 3 m s^{-1}. Upper panels correspond to a screen with SC=34.8% and the lower panels to SC=64%.

8.3. Angle of inclination of the row of filaments

Theoretical and experimental results indicate that the angle of inclination of filaments affects the fog water collection ability. The explanation is rather complex due to different concomitant effects. Changes in the angle of attack of the wind stream affect the Stokes number, i.e. the impaction, but also the aerodynamic efficiency. Additionally, the drag forces exerted on the pinned drops vary depending on the tilting of the screen. The cross-sectional area exposed to the wind flow decreases with the angle of inclination and therefore presumable improvements in the collection rate of a yawed screen must be balanced with such a loss in collection surface. In order to test the possibility of maximising the fog water collection yield by inclining the screen, the optimum spacing arrangement discussed above (SC=34.8%) was tilted from 60° to -60° in steps of 15° with respect to the vertical in a series of experiments carried out in the wind tunnel (Fig. 34). Tilting the screen either in the direction of air flow (positive angle) or countercurrently (i.e. negative angles) decreased the water collection due to the loss in cross-sectional area (cf. orange and grey symbols in Fig. 35). The yield was more than 1.5-fold at ±60° with respect to that obtained with the screen positioned vertically (0°), if the reduction in vertical area is corrected (orange symbols in Fig. 35). Small tilting angles (< 30°) did not suppose a significant reduction of fog water collection, despite the decline in orthogonal projected area.

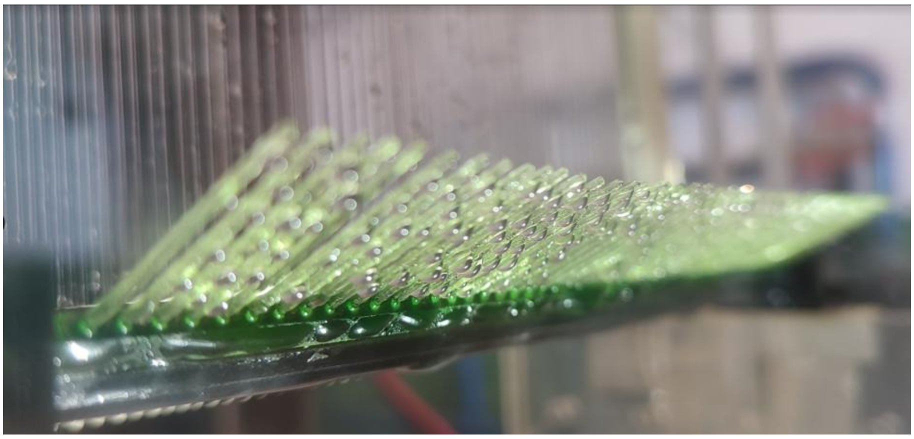

Fig. 34. An inclined screen inside the wind tunnel test chamber where pinned fog water drops may be observed.

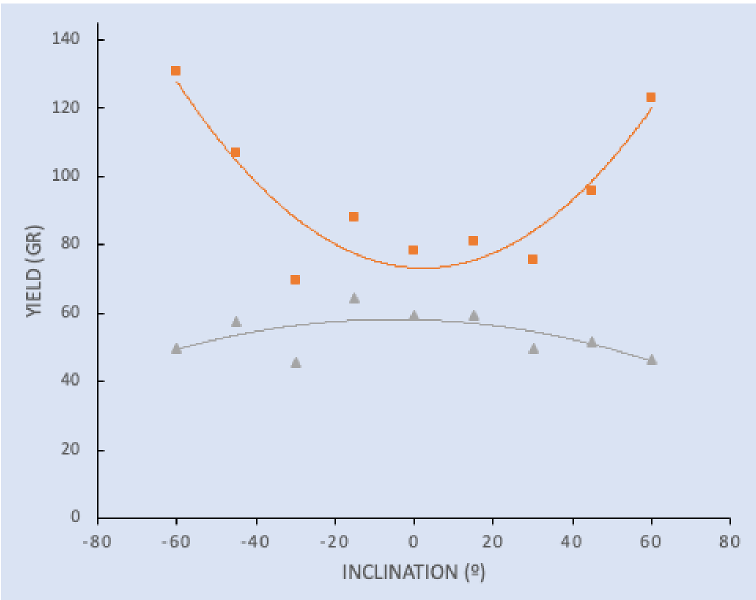

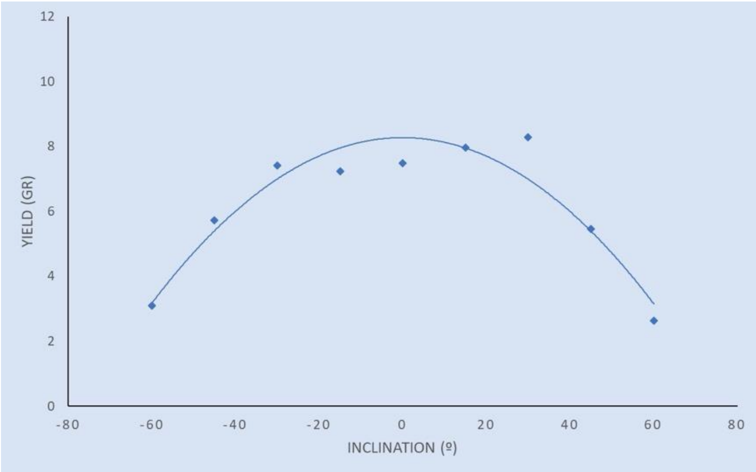

Fig. 35. Dependence of the fog water yield of the screen with the angle of inclination. Angles are referred with respect to the vertical (0°). Positive signs indicate orientation in the direction of the air flow while negative values correspond to tilting the screen counter-currently. Orange symbols refer to yields after correcting per cross-sectional vertical area. Top: experiments carried out with two fog systems in parallel, i.e. ChillBooster and Humisonic, and therefore a wide range of droplet diameters (1-50 µm); bottom: experiments carried out solely with the Humisonic fog system, i.e. small (1-5 µm) fog water droplets.

8.4. Number of rows

An arrangement of parallel fibres, as the one discussed so far, permits rapid evacuation of pinned drops and minimises clogging due to the absence of crosslinked intersections where water films adhere. However, the shading coefficient (SC) halves with respect to an intertwined screen comprising both vertically and horizontally oriented filaments. The impaction efficiency is affected by the SC, reaching a maximum beyond which aerodynamical effects come into play (Figs. 32, 33). One way of increasing the SC is by placing different staggered filament rows in parallel (Fig. 36). We expect that this would promote the impaction of droplets without significantly affecting the aerodynamical efficiency. Fog water droplets scaping the first row would be captured by subsequent ones further downwards and thus the collection of fog water may be improved. The results shown in Fig. 37 confirm this. Water yield was 1.5-times higher as the number of impacting screens increased from 1 up to 4. However, no much improvement was achieved beyond the second layer, such that the fog water collection levels off up to a plateau after this. Therefore, from the point of view of cost and manufacturing, more than 2-3 rows do not seem to represent much extra benefits. The experimental results were verified numerically via CFD simulations (Fig. 38).

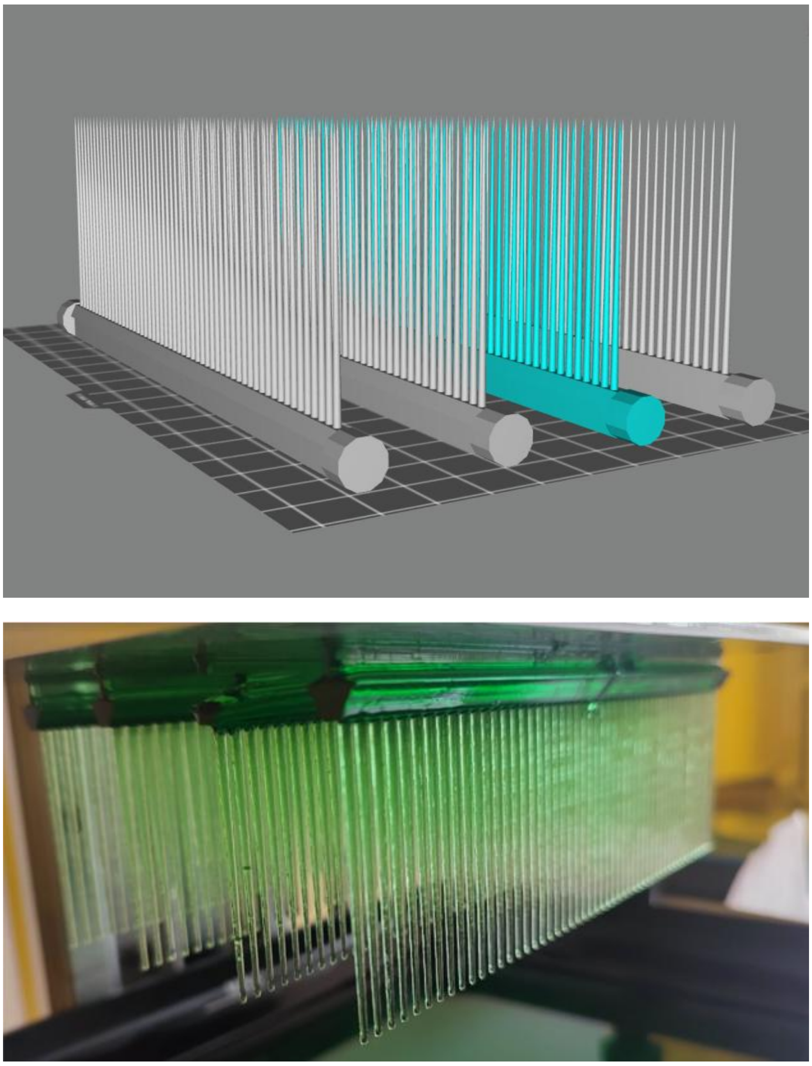

Fig. 36. Designed (top) and 3D printed array of four parallel screens.

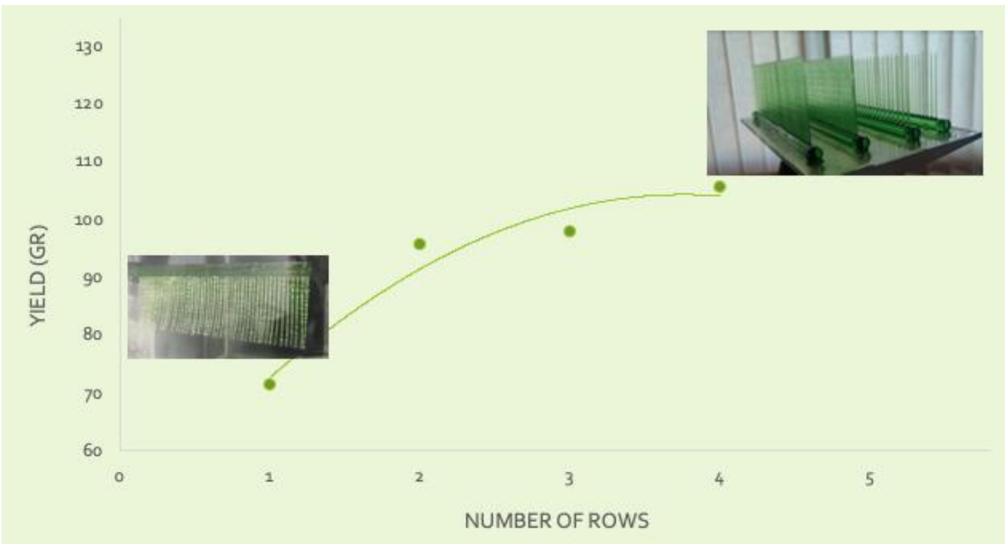

Fig. 37. Variation in the fog water yield with the number of parallel screen rows.

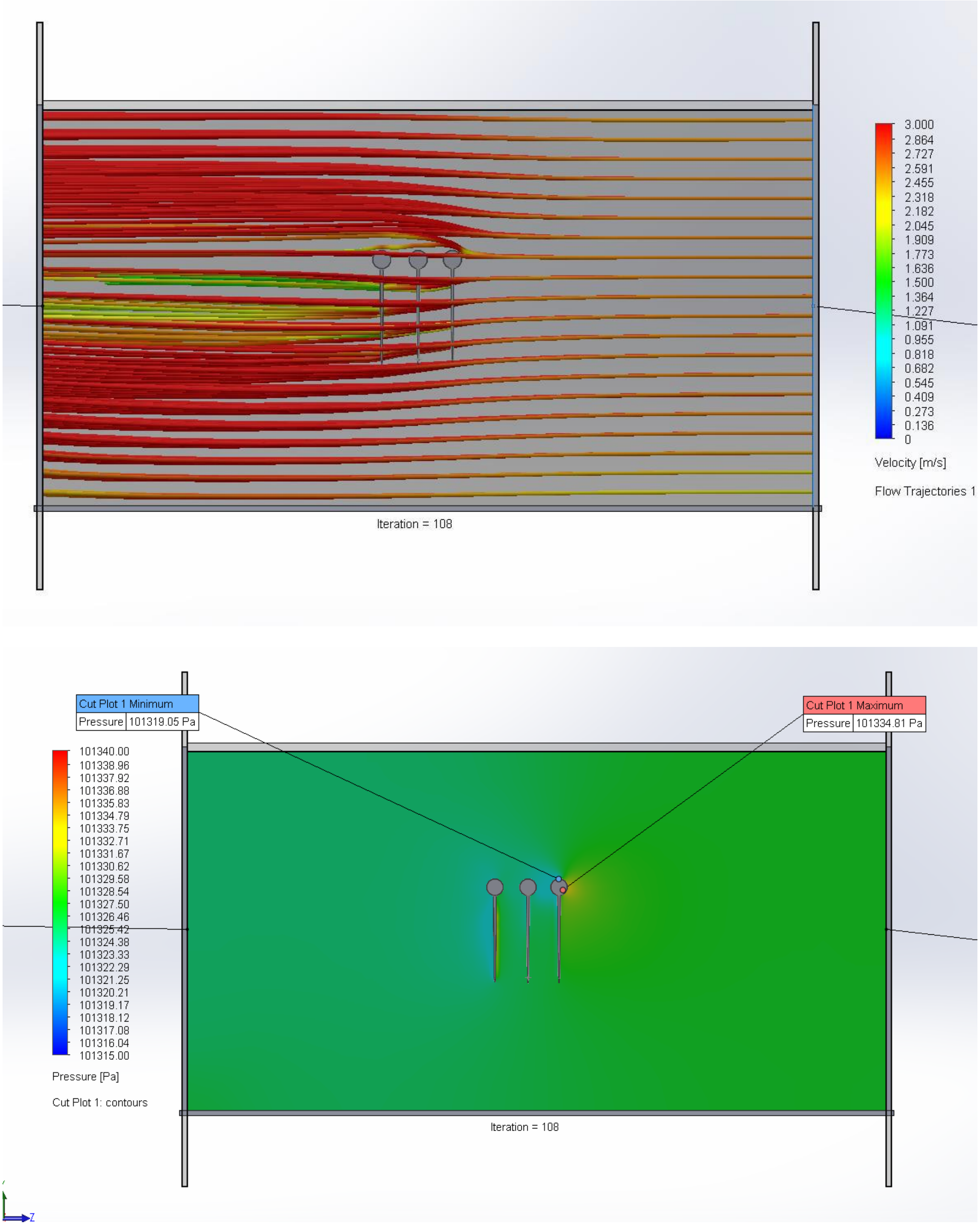

Fig. 38. Numerical simulations of a three-layer flat screen inside the test chamber. Cross-sectional view of the trajectories and velocity field (top); pressure field (bottom) at wind speed of 3 m s^{-1}.

8.5. Curvature of the screen

Theoretical results indicate that the curvature of the screen affects the aerodynamics via the drag coefficient of a blunt object, and that concave screens are more aerodynamically efficient. Consequently, different C-shape geometries, either concave or convex (Fig. 39), were tested in the wind tunnel and yields were compared with a flat screen. Note, however, that C-shape screens have a larger perimeter (that is, a greater number of filaments and therefore larger shading coefficient) than a flat screen with equivalent frontal area perpendicular to the wind. Thus, we compared C-shape and flat geometries with both equal shading coefficient (SC=35%), that is, same number of filaments unequally spaced (Fig. 40), and with constant separation distance of filaments (2.7 mm) and therefore different SC=56%. The results show that, although collection yield increased with the screen curvature (either concave or convex), this improvement was compensated if corrected by the number of filaments (i.e., equal projected shading) (Fig. 41). Furthermore, a curved screen also occupies a higher ground area (diameter × radius), and thus it results more advantageous to cover the same space with parallel staggered flat screens, as discussed in the previous section. This decision was also taken based on CFD numerical simulations of a three-layer concentric concave arrangement (Fig. 42).

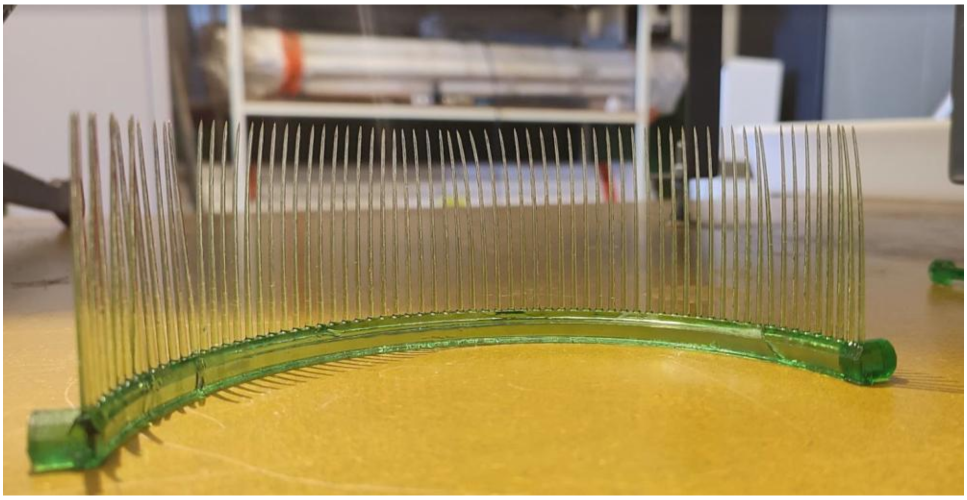

Fig. 39. An example of a 3D-printed concave screen used to study the effect of curvature on the fog water yield.

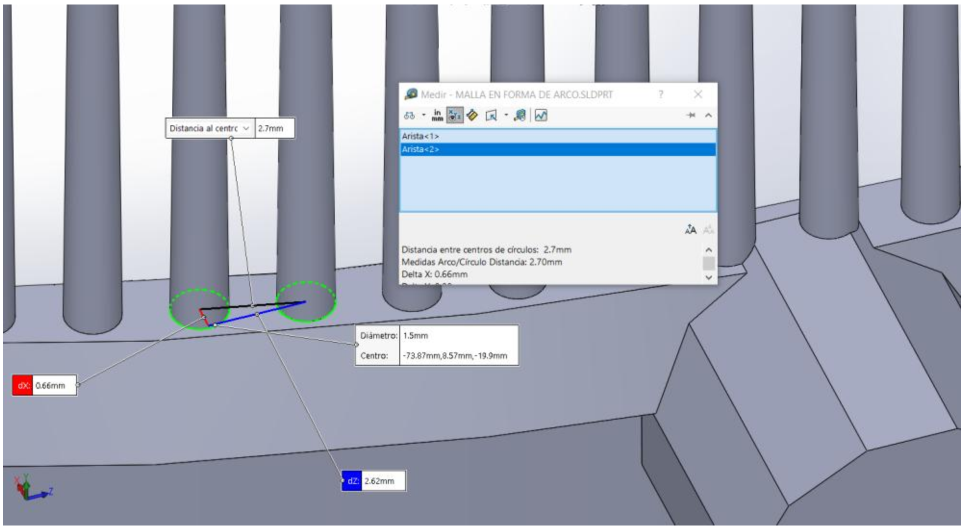

Fig. 40. Redesign of a curved screen in order to accommodate variable separation distances between filaments and therefore a projected shading coefficient equivalent to a flat geometry.

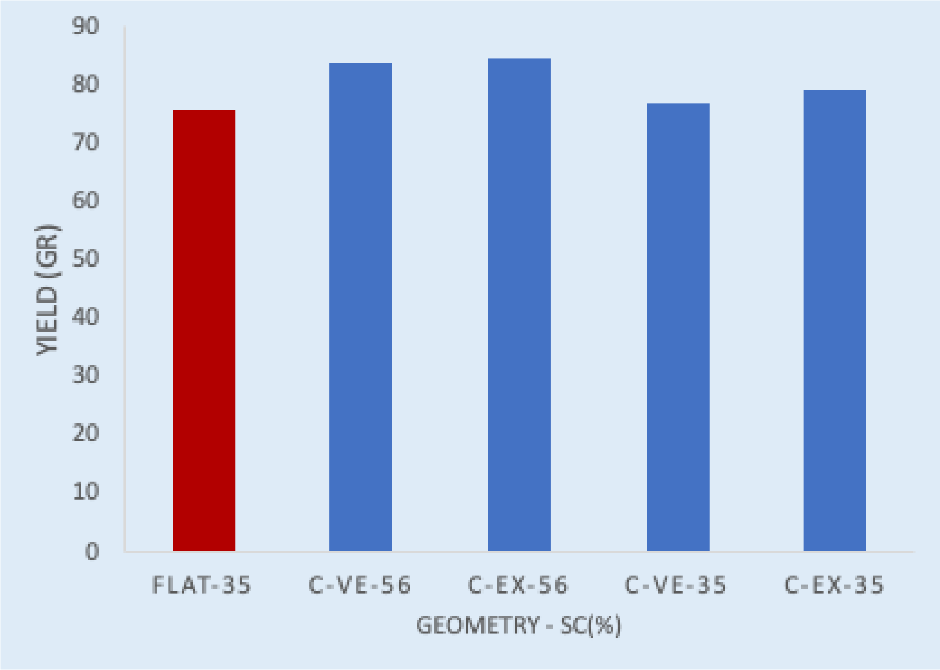

Fig. 41. The effect of curvature, i.e. concave (C-VE) and convex (C-EX), with both equal (SC=35%) and non-equal (SC=56%) shading coefficient, with respect to a flat screen (red bar) on the fog water yield.

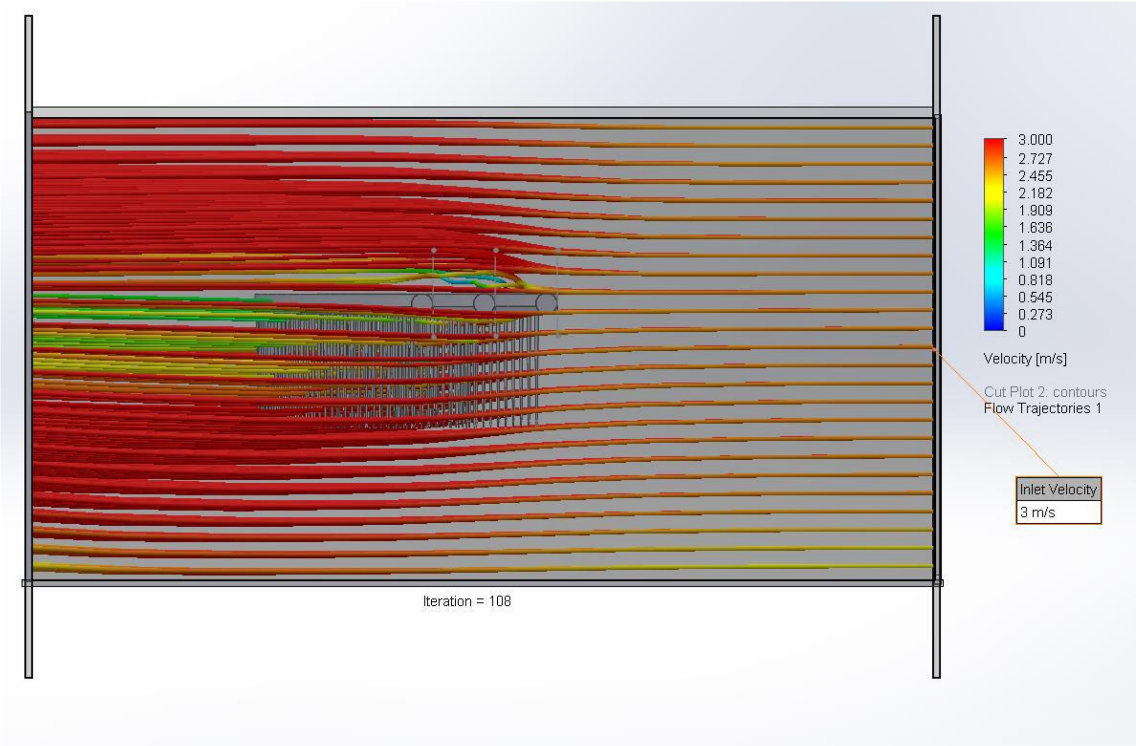

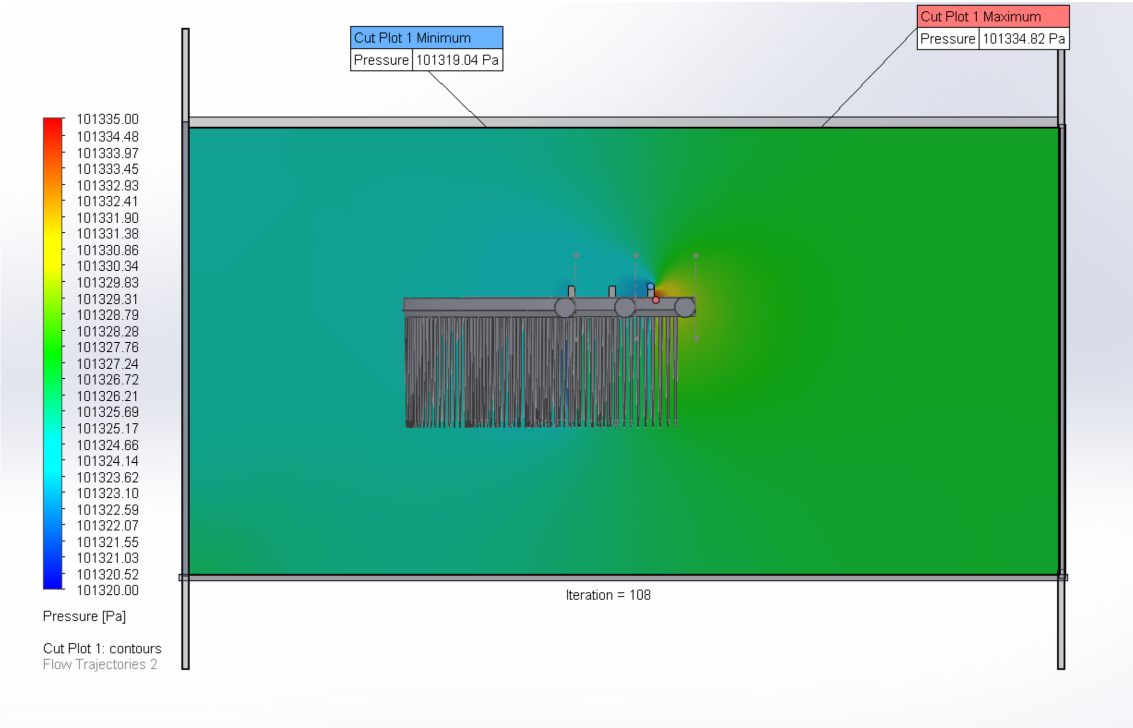

Fig. 42. Numerical simulations of a three-layer concave screen inside the test chamber. Cross-sectional view of the trajectories and velocity field (top); pressure field (bottom) at wind speed of 3 m s^{-1}.

8.6. Ladder-like arrangement of the prototype

With all the information gathered in the multiple experiments carried out and discussed in previous sections, we designed a prototype of the fog water collector that includes the optimal features of the different aspects investigated: shading, number of screens, inclination, curvature, etc. As already commented in section 4, a ladder-like 3D-structure was proposed in order to solve many of the inconveniences of traditional FWC. However, in order to be able to test this 3D prototype inside the wind tunnel, some modifications had to be carried out in the test chamber. In particular, the lower methacrylate side of the chamber had to be replaced by some kind of collecting surface that permits channelling all the water dripping from the 3D ladder. We opted for an inclined ramp that drips into a gutter below. Firstly, we carried out different numerical simulations, in order to study the effect of this new element on the air flow and what disposition of the ramp would be the least disturbing (Fig. 43).

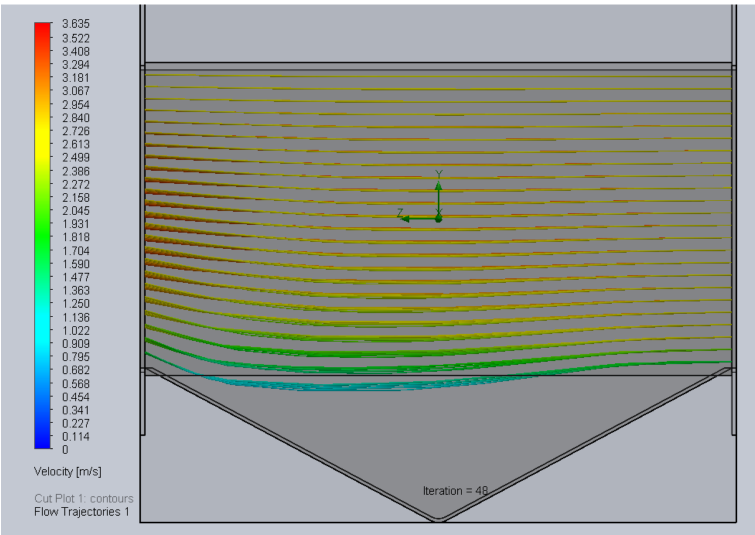
3.635
3.522
3.408
3.294
3.181
3.067
2.954
2.840
2.726
2.613
2.499
2.386
2.272
2.158
2.045
1.931
1.818
1.704
1.590
1.477
1.363
1.250
1.136
1.022
0.909
0.795
0.682
0.568
0.454
0.341
0.227
0.114
0
Velocity [m/s]
Cut Plot 1: contours
Flow Trajectories 1
Iteration = 48

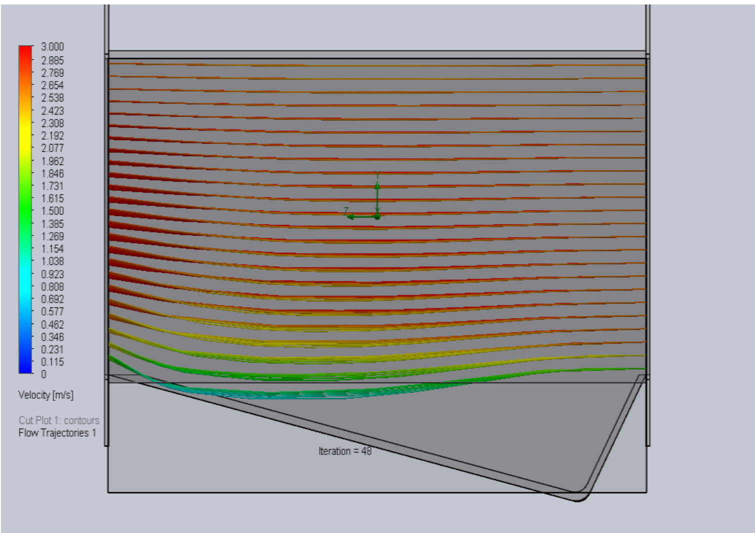
3.000
2.885
2.769
2.654
2.538
2.423
2.308
2.192
2.077
1.962
1.846
1.731
1.615
1.500
1.385
1.269
1.154
1.038
0.923
0.808
0.692
0.577
0.462
0.346
0.231
0.115
0
Velocity [m/s]
Cut Plot 1: contours
Flow Trajectories 1
Iteration = 48

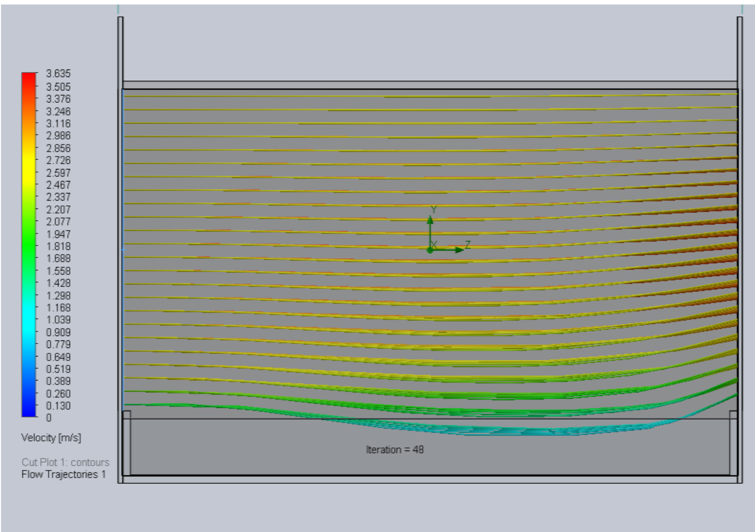
3.635
3.505
3.376
3.246
3.116
2.986
2.856
2.726
2.597
2.467
2.337
2.207
2.077
1.947
1.818
1.688
1.558
1.428
1.298
1.168
1.039
0.909
0.779
0.649
0.519
0.389
0.260
0.130
0
Velocity [m/s]
Cut Plot 1: contours
Flow Trajectories 1
Iteration = 48

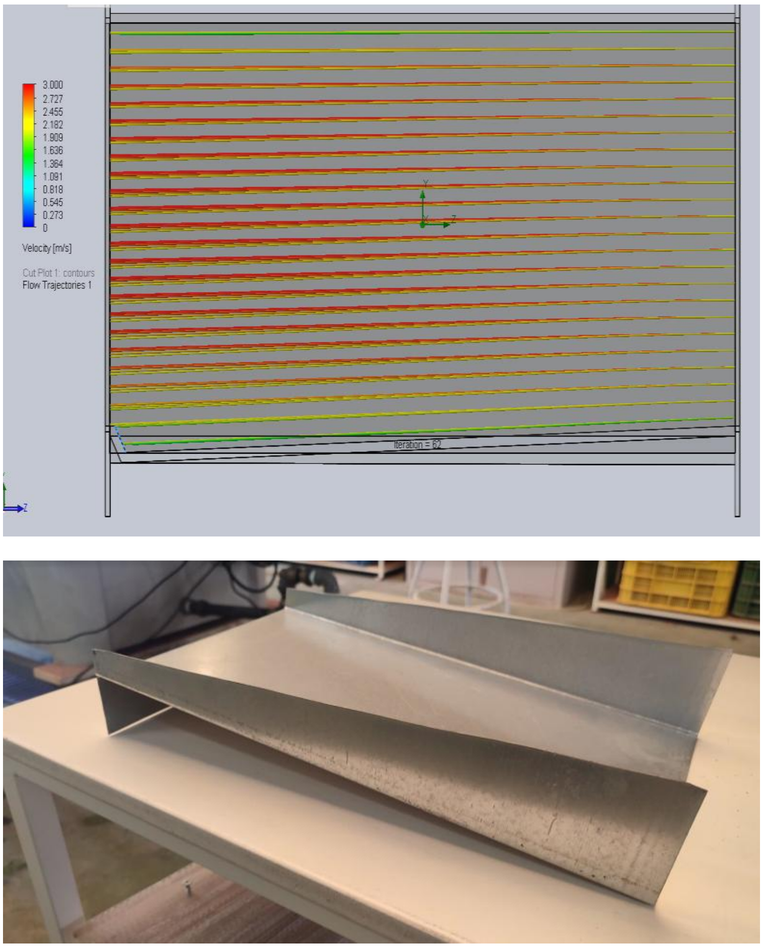

Fig. 43. Numerical simulations to investigate the flow disturbance as a consequence of modifications of the lower side of the wind tunnel test chamber. From top to bottom: pyramidal, skewed pyramid, flat and inclined. Final design fabricated based on the simulations.

The simulations indicated that a ramp inclined in the direction of the air current and open at the other end would be the least flow disturbing disposition. A flap was added on the final end to facilitate the dripping of water into the gutter below (Fig. 44).

Fig. 44. Detail of collecting ramp, dripping in the gutter below, fabricated to replace the lower side of the test chamber in the wind tunnel.

After these modifications in the wind tunnel chamber, we proceed to test the FWC prototypes. We designed and 3D printed different versions by varying the number of parallel rows (1-3) and the inclination of the filaments (perpendicular versus 45°) in order to evaluate their performance (Fig. 45).

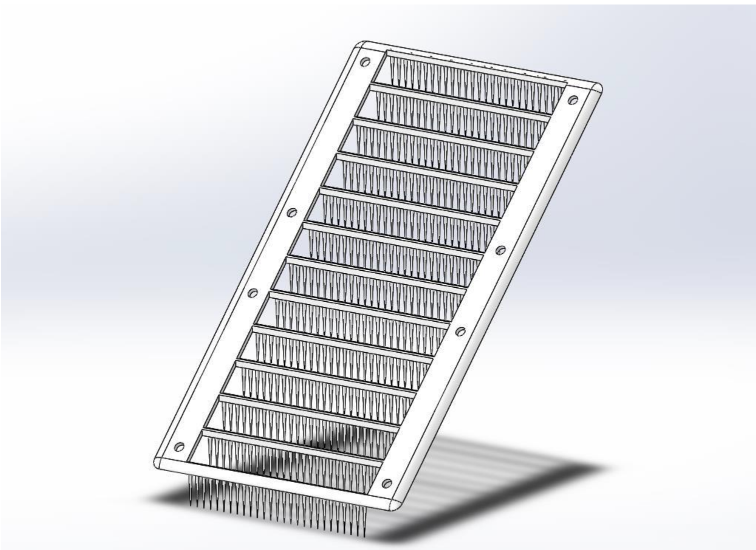

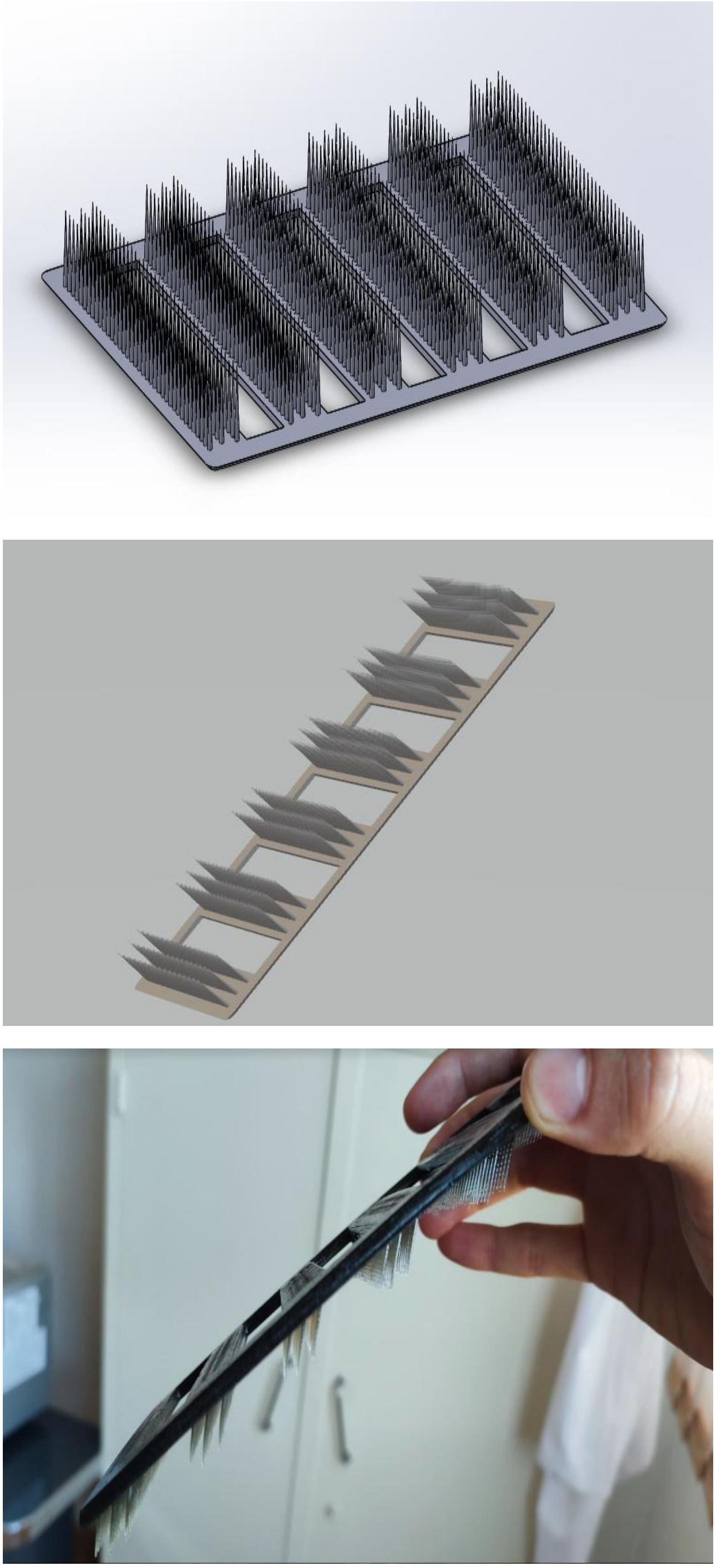

Fig. 45. Examples of the different FWC prototypes designed and 3D printed.

After many iterations we arrived to a final i-FWC prototype that includes many of the optimal features of the tested designs combined with simplicity and robustness of the structure: a multilayer of vertical conical filaments supported by an open frame (Fig. 46).

Fig. 46. From top to bottom: final FWC prototype designed, 3D printed and tested in the wind tunnel.

The prototype was tested in the tunnel (Fig. 46) at different wind speeds and efficiencies were estimated to be 10-20% with a maximum at 5 m s^{-1} (Fig. 47)

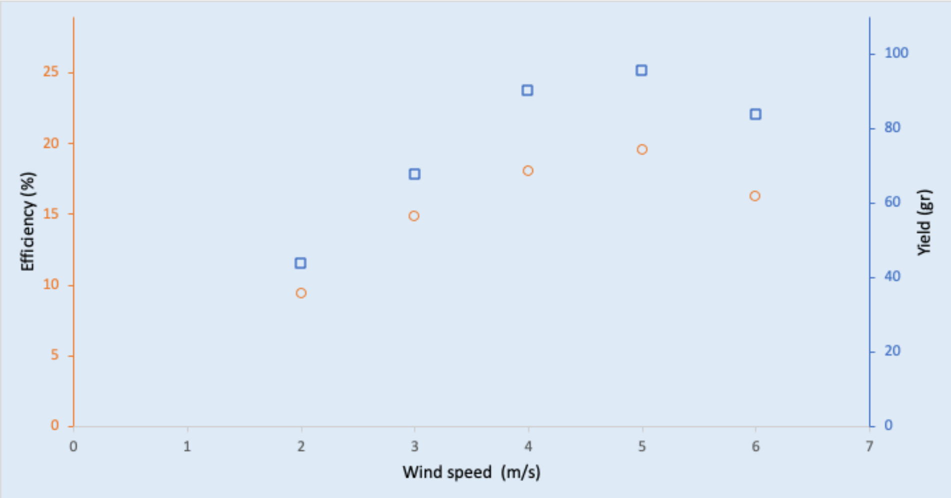

Fig. 47. Variation with the wind speed of the fog water yield (blue squares; right hand side axis) and efficiency (orange circles; left hand side axis) of the FWC prototype inside the wind tunnel.

10. The innovative fog water collector (i-FWC)

9.1. Moving from the lab to the field: construction of the i-FWC 1.0

The 3D printing technique permitted us to rapidly fabricate *ad hoc* prototypes to test their performance in the lab. Once a final design was achieved, moving from the small-scale laboratory "toy" FWC to larger field deployable collectors was challenging. Issues of large-scale production, cost, material availability, viable manufacturing method, etc. arose, then. This was a long process of searching, consulting and testing with different companies that took us over two months of work. A summary of the different possibilities evaluated is included in Appendix IV. We arrived to the final conclusion that commercial metallic anti-clogging meshes employed in the food, mining quarry, and aggregate processing industries would be a viable alternative that meet our requirements: certain degree of *ad hoc* fabrication, resistance to harsh conditions, contained cost, commercial availability, etc. Anti-clogging screen meshes are made of horizontally crimped round wires of different spacing geometry and filament dimensions. The in-catalogue screen that closely matched our 3D printed prototype was that with a rectangular mesh opening (1.5 mm × 50 mm) and cylindrical filaments of diameter ∅=1.25 mm rendering a 53% shading coefficient. This was the commercial screen with characteristics closest to those of the prototype we could find (Fig. 48).

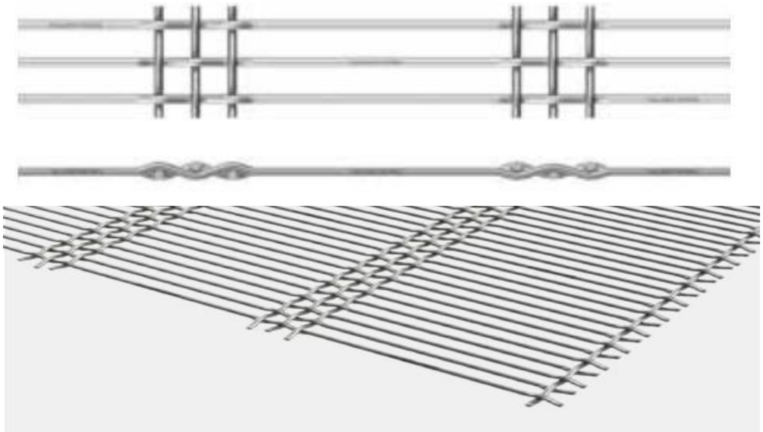

Fig. 48. Anti-clogging metallic screen selected for the construction of the field deployable i-FWC.

A similar arrangement to that of the anti-clogging screen was hand-made using an array of metallic filaments and was tested in the wind tunnel, in order to evaluate its overall performance, and in particular the fact that metallic and not resin-based material may have different wetting behaviour (Fig. 49).

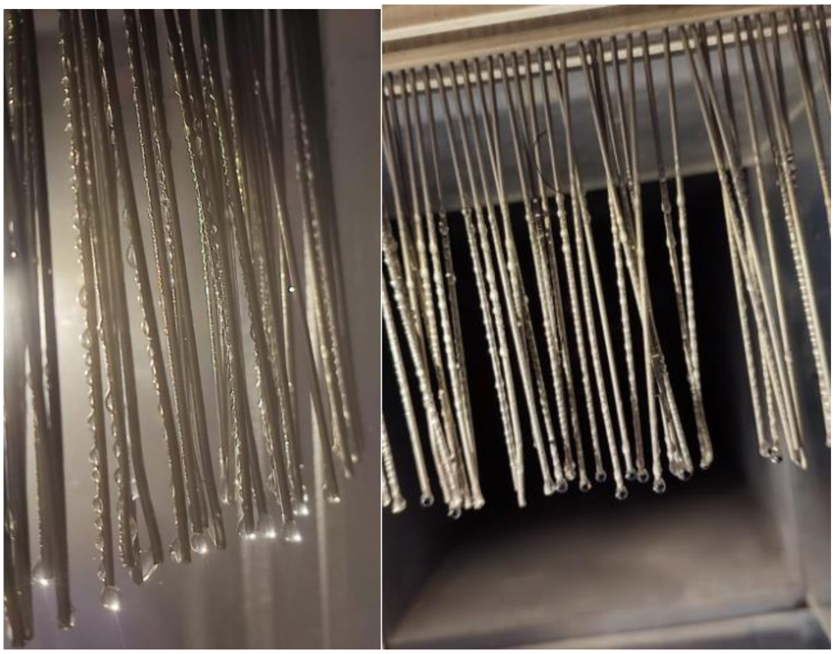

Fig. 49. Wind tunnel experiment with an equivalent arrangement of metallic strings to that of the anti-clogging screen.

Once we confirmed a satisfactory behaviour of this type of metallic material, we planned to build the i-FWC for field deployment by either sectioning or folding the anti-clogging screen to arrive to the design originally envisioned (Fig. 1). The process is schematically illustrated in Fig. 50.

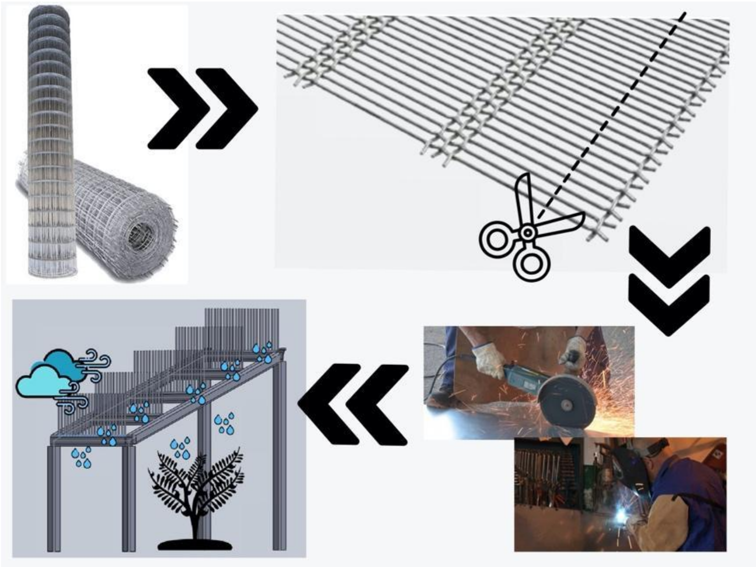

Fig. 50. Schematic illustration of the process to be followed for building the final deployable i-FWC 1.0.

The structural design of the i-FWC 1.0 has been based on biomimetics principles and, in particular, the fog basking capabilities of the Namib desert beetles. We have also taken into consideration issues related to its easy-deployment in the field, self-ground-sustenance and portability, so we have built a structure that is removable and light to carry (Fig. 51). Numerical simulations were also carried out to verify that the structure would support sustained strong winds (> 100 km h^{-1})

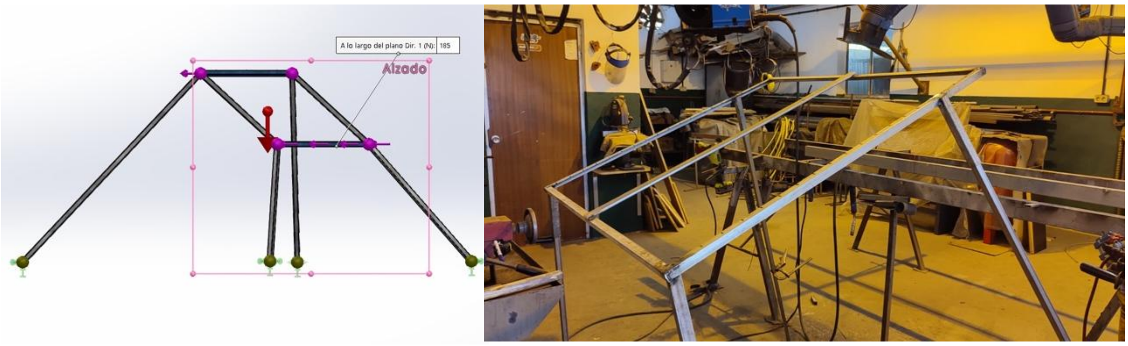

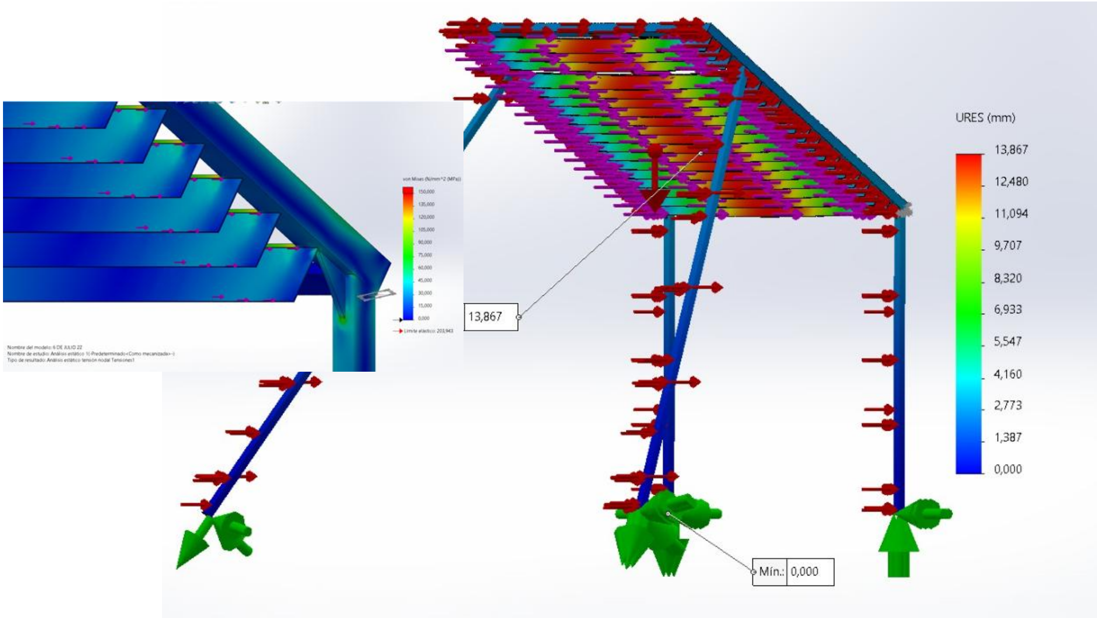

Fig. 51. Design and construction of the support structure of the i-FWC 1.0. Simulations were carried out to verify that the structure would stand strong wind gusts.

9.2. Construction, field deployment and testing of i-FWC 2.0

The mesh was sectioned in 1 m long strips of 6.5 cm width. These were welded to a 1 m × 1 m frame in 19 parallel rows 5 cm apart. The frame was inclined 33º and joined to four supporting vertical square bars of galvanized steel in its corners. In its upper part the i-FWC is 1.65 m tall and 1.10 m at the lowest. A collecting tray was placed below and water was diverted to a container through pipe connections (Fig. 52). The whole structure was fixed to the ground with anchor-spikes that were hammered in the terrain and were attached to the four legs of the i-FWC structure with U-bolt grips. This facilitated field installation without the need of concrete foundations, although these may be required if the soil structure is loose (Fig. 53). The whole FWC weights less than 20 kg. The cost of each i-FWC is in the range of 1000-1200 € depending on materials used, construction contracts and/or units of i-FWC fabricated (i.e. more collectors would reduce the costs per unit). A detailed description of the devised i-FWC, its mounting and field installation procedure are available at www.lifenieblas.com/sites/default/files/documentacion/2023/MANUAL%20MODULAR%20i-FWC%20%2B%20BLUEPRINTS.pdf.

Fig. 52. Construction of the i-FWC 2.0 units at the ICIA workshop.

Fig. 53. Field deployment of i-FWC 2.0 units below the t-FWC in El Pinillo (Valleseco, Gran Canaria).

9.3. Improvements of the fog water collector after first field initial trial: i-FWC 2.1

Some issues related to leaking and structural compliance of the water collecting tray arose during the first field campaign (Fig. 54). These issues were resolved in a new version of the fog water collector i-FWC 2.1. The original polycarbonate tray was replaced by one fabricated with galvanised steel without much comprising lightness of the FWC and the sink valve was moved to the center (instead of the corner as in the i-FWC 2.0) to facilitate evacuation of the collected water. The tray was fixed to the FWC structure through square tubes welded on its outer sides at the insertion distances of the four legs where it is screwed. This served two purposes: one, to avoid water leaking on the sides of the tray and two, to facilitate field mounting by providing a template for the correct insertion of the vertical legs (Fig. 55).

Fig. 54**.** Water leaking and tray breakage issues observed in the field deployed i-FWC 2.0.

Fig. 55. The upgraded version of the fog water collector (i-FWC 2.1) being installed in the field, showing the improved collecting tray.

9.4. Modularity of the i-FWC

An important aspect of fog water collectors is their potential to being scaled up and their modularity. These issues were explored by designing a 2 $\times$ 4 modular version of the i-FWC that was deployed and tested in the field (Fig. 56).

Fig. 56. Modular i-FWC being installed in El Pinillo (Valleseco, Gran Canaria).

9.5. Comparison of i-FWC with other fog water collectors

The fog water yields of the devised i-FWC were compared with other 3D FWCs installed at the site. These consist of a parallelepipedal structure of galvanized steel: 2 m (L) × 0.5 m (W) × 4 m (H). Nine units were covered on all their sides by a single layer of a plastic mosquito net (shading coefficient, SC=38%) and three internal hanging curtains of the same mosquito net equidistantly spaced. In the forthcoming we will refer to this type of collector as "traditional" or t-FWC (Fig. 53). For comparison purposes, three extra units were covered only on the front wind exposed side, with a so-called volumetric geotextile, that has been suggested to be more efficient than other traditional textiles. We employed the polypropylene BonTmat mesh (SC=50%) from Objetivo Erosionzero, S.L. (www.controlerosion.es). Hereinafter we will refer to this type of collector as "volumetric" or v-FWC (Fig. 57). All FWCs were oriented to the dominant wind direction in a slopy exposed area.

Each type of FWC was connected in series and the joint collected fog water volumes were measured with a flowmeter (MTKD-M DN 32, ZENNER International GmbH & Co.) associated to an electronic pulser. Temporal discontinuities in the fog water input and the low volumes to be measured would make such discrete readings with the flowmeters unreliable. Thus, to prevent this to occur, water volumes were accumulated upstream in a 35 L tank equipped with an autonomous discharge system prior to the flowmeter. As a double check of the reliability of the flowmeter data and in case of sporadic failures, cumulative water volumes were also registered manually on a daily basis by measuring the water height in the 1000 L deposits installed at the end of the line.

Fig. 57. Traditional fog water collector (t-FWC) where the mosquito screen (green) is being replaced with a volumetric textile (v-FWC).

9.6. Fog water yields of the different FWCs

The distribution of fog water volumes collected by the three FWCs was analyzed during a two-year period from 20th September 2022 until 20th august 2024. Fog was collected mainly outside the summer period, which was also the driest period in terms of precipitation (Fig. 58). Average daily fog water yields differed between the three FWCs, with the i-FWC rendering the highest values, followed by the v-FWC and the t-FWC. The mean i-FWC yield was almost double of that of the v-FWC and nearly four times that of t-FWC (Fig. 59). Since the 3D supporting structure of the v-FWC and t-FWC is the same, the higher yields of the former may be explained in terms of the screen used in each case. Among possible explanations for the lower performance of the mosquito mesh we may stress that its small pore openings (1.5×1.5 mm) may lead to clogging and adhesion of pinned drops, thus hindering their gravitational removal and affecting the screen aerodynamical efficiency, that would behave as a blunt body instead. By contrast, in the volumetric mesh, despite its higher SC (50% vs. 38%), pores are not homogenously distributed and present larger ones in different z-planes, that favor the air cross-flow while providing a greater impaction area. Notice also that, although the t-FWCs have additional multilayers of the mosquito screen that would presumably increase the collection efficiency, this did not seem to contribute much to their fog water yield. With respect to the superior performance of the i-FWC we may comment on the harp-like distribution of filaments, less prone to clog); their multilayer disposition, that increases the probability of droplet impaction; and the short length of the filaments, that facilitates fast evacuation of drops. Furthermore, the i-FWC support structure is open and permeable, which would presumably represent a small obstruction to crosswind flow while being structurally stable.

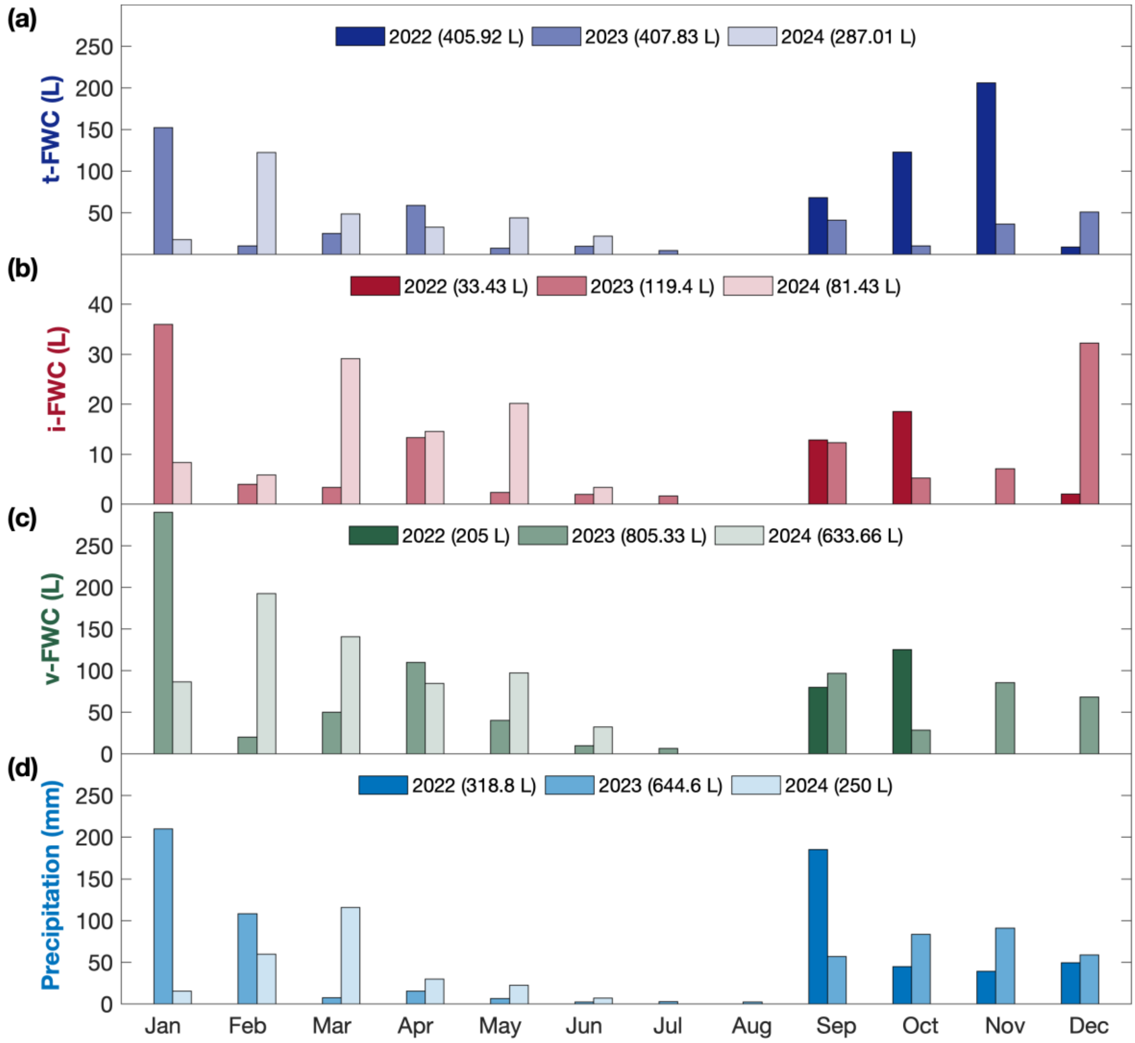

Fig. 58. Monthly distribution of fog water volumes collected by three FWCs (a-c) and precipitation (d) during a two-year period.

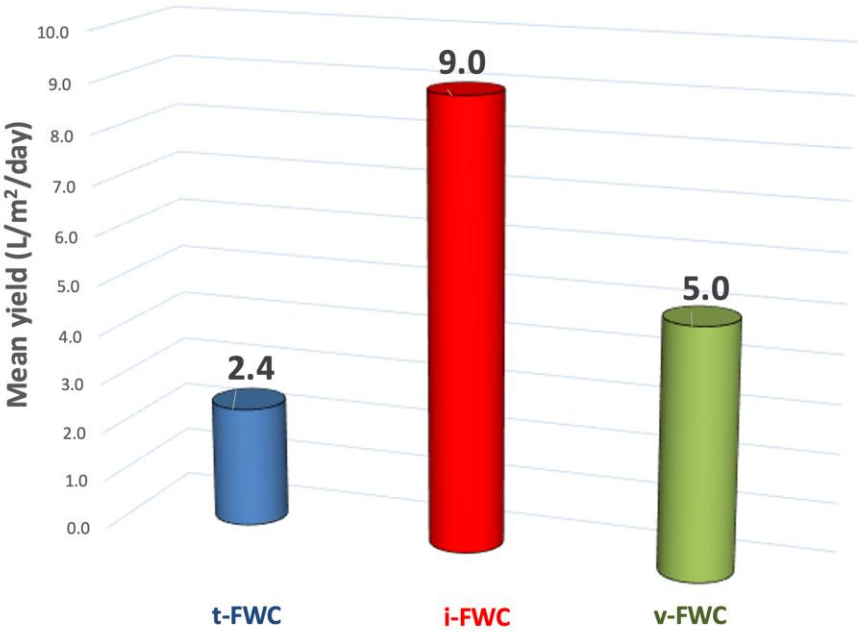

Fig. 59. Mean daily fog water yields of the three FWCs tested.

11. Conclusions

Most innovations in fog water collection do not pass the prototype or lab phase, not reaching field testing in real applications. Impracticality of the design, unavailability of the construction materials and cost are among the main reasons to blame in the short span. In the long term, fog projects mainly fail because structural malfunctions lead to breakage and collapse of FWCs and, consequently, abandonment. We upscaled using readily available materials a FWC model previously tested under lab conditions. We displayed a series of 21 units in the field and compared their fog water yields with other three-dimensional FWCs. The devised i-FWC showed better performance than the other two collectors with mean daily yields up to four-fold that of the t-FWC and almost double of the v-FWC. There is room for future improvements though. Among these we may mention a further cost reduction achievable by mass production. For this to occur, further applications of the proposed design around the World under different conditions and scenarios are needed to confirm the early results here obtained. To promote this, blueprints and manufacturing instructions have been made available for the public in the web portal of the Life Nieblas project. Improvements may also come from a screen design with a shading coefficient and filament diameter closer to the optimum obtained under lab conditions. This again implies involvement of the industry to mass produce the desired screens. This will only come if further projects strengthen the advantages of the collector devised and make it profitable. Although improved efficiency is an important issue to take into account, lower yields may be compensated by increasing the impaction area of the FWC. This is at the expense of making the structure more prone to collapse though, a concern that is particularly relevant in large 2D FWCs. Also cost and field installation, particularly transportation to remote areas and foundations, are compromised. We have tackled the stability issues of the devised FWC by translating a 2D impaction surface into an equivalent more stable 3D assembly, while fog water yields have been enhanced. The structure is also modular, lightweight and easy to deploy in the field.

Authors:

Dr. Carlos M. Regalado - cregalad@icia.es

Carlos Fariña – cfarina@icia.es

Dr. Alfredo Reyes – areyes@icia.es

Norberto González - nrguezg@icia.es

Fermín Correa – fcorrea@icia.es

Acknowledgements:

We thank the Spanish Agency Aeropuertos Españoles y Navegación Aérea (AENA) for allowing access to their facilities in Taborno and to Sieltec Canarias S.L. for their technical support.